Identification and Interaction Analysis of Molecular Markers in Pancreatic Ductal Adenocarcinoma by Bioinformatics and Next-Generation Sequencing Data Analysis

Bioinformatics and Biology Insights
Volume 17: 1–34

DOI: 10.1177/11779322231186719

Muttanagouda Giriyappagoudar, MD[1], Basavaraj Vastrad, PhD[2], Rajeshwari Horakeri, PhD[3] and Chanabasayya Vastrad, PhD[4]

[1]Department of Radiation Oncology, Karnataka Institute of Medical Sciences (KIMS), Hubballi, India. [2]Department of Pharmaceutical Chemistry, K.L.E. Society's College of Pharmacy, Gadag, India. [3]Department of Computer Science, Government First Grade College, Hubballi, India. [4]Biostatistics and Bioinformatics, Chanabasava Nilaya, Dharwad, India.

ABSTRACT

BACKGROUND: Pancreatic ductal adenocarcinoma (PDAC) is one of the most common cancers worldwide. Intense efforts have been made to elucidate the molecular pathogenesis, but the molecular mechanisms of PDAC are still not well understood. The purpose of this study is to further explore the molecular mechanism of PDAC through integrated bioinformatics analysis.

METHODS: To identify the candidate genes in the carcinogenesis and progression of PDAC, next-generation sequencing (NGS) data set GSE133684 was downloaded from Gene Expression Omnibus (GEO) database. The differentially expressed genes (DEGs) were identified, and Gene Ontology (GO) and pathway enrichment analyses were performed. The protein-protein interaction network (PPI) was constructed and the module analysis was performed using Integrated Interactions Database (IID) interactome database and Cytoscape. Subsequently, miRNA-DEG regulatory network and TF-DEG regulatory network were constructed using miRNet database, NetworkAnalyst database, and Cytoscape software. The expression levels of hub genes were validated based on Kaplan-Meier analysis, expression analysis, stage analysis, mutation analysis, protein expression analysis, immune infiltration analysis, and receiver operating characteristic (ROC) curve analysis.

RESULTS: A total of 463 DEGs were identified, consisting of 232 upregulated genes and 233 downregulated genes. The enriched GO terms and pathways of the DEGs include vesicle organization, secretory vesicle, protein dimerization activity, lymphocyte activation, cell surface, transferase activity, transferring phosphorus-containing groups, hemostasis, and adaptive immune system. Four hub genes (namely, cathepsin B [CCNB1], four-and-a-half LIM domains 2 (FHL2), major histocompatibility complex, class II, DP alpha 1 (HLA-DPA1) and tubulin beta 1 class VI (TUBB1)) were obtained via taking interaction of different analysis results.

CONCLUSIONS: On the whole, the findings of this investigation enhance our understanding of the potential molecular mechanisms of PDAC and provide potential targets for further investigation.

KEYWORDS: Pancreatic ductal adenocarcinoma, bioinformatics analysis, biomarker, enrichment analysis, differentially expressed genes, next-generation sequencing

RECEIVED: January 12, 2023. **ACCEPTED:** June 18, 2023.

TYPE: Original Research Article

FUNDING: The author(s) received no financial support for the research, authorship, and/or publication of this article.

DECLARATION OF CONFLICTING INTERESTS: The author(s) declared no potential conflicts of interest with respect to the research, authorship, and/or publication of this article.

CORRESPONDING AUTHOR: Chanabasayya Vastrad, Biostatistics and Bioinformatics, Chanabasava Nilaya, Bharthinagar, Dharwad 580001, Karnataka, India. Email: channu.vastrad@gmail.com

Introduction

Pancreatic ductal adenocarcinoma (PDAC) is a type of cancer that arises from the cells lining the pancreatic ducts.[1] Epidemiological studies have identified several risk factors for PDAC, including age, sex, smoking, chronic pancreatitis, obesity, diabetes, family history, and occupational exposure.[2] In terms of incidence, PDAC is the 12th most common cancer in the world, accounting for about 2% of all cancers. However, it is the seventh leading cause of cancer death, responsible for about 5% of all cancer deaths.[3] Despite new developments in multimodal therapy, its overall 5-year survival rate remains less than 8%.[4] Hemostasis is the process that stops bleeding,[5] and immunity refers to the body's defense mechanism against foreign substances, including cancer cells.[6] Pancreatic ductal adenocarcinoma (PDAC) is associated with alterations in both hemostasis and immunity. Pancreatic ductal adenocarcinoma treatment commonly includes surgery, radiation, chemotherapy, and immunotherapy.[7] However, PDAC remains common and malignant due to recurrence and metastasis, and is ultimately key cause of PDAC-associated death.[8] Therefore, there is a vital need to advance new diagnostic strategies and therapeutic agents to upgrade the prognosis of patients with PDAC.

The molecular mechanisms of PDAC tumorigenesis and development remain imprecise. It is, therefore, key to identify novel genes and pathways that are linked with PDAC tumorigenesis and patient prognosis, which might not only help to illuminate the underlying molecular mechanisms involved but also to disclose novel diagnostic markers and therapeutic

targets. Some of the key genetic alterations that have been implicated in PDAC include mutations in the KRAS proto-oncogene, GTPase (KRAS), tumor protein p53 (TP53), cyclin-dependent kinase inhibitor 2A (CDKN2A), SMAD family member 4 (SMAD4) and BRCA2 DNA repair–associated (BRCA2) genes. These mutations can occur in various combinations, and their precise roles in PDAC are still being studied.[9] Oji et al[10] demonstrated that the overexpression of WT1 is linked with prognosis in patients with PDAC. A previous investigation reported that phosphoinositide 3-kinase signaling pathway is linked with development of PDAC.[11] Next-generation sequencing (NGS) can promptly uncover gene expression on a global basis and is especially useful in identifying for differentially expressed genes (DEGs).[12] A huge amount of data have been generated through the use of NGS and the majority of such data have been deposited and saved in public databases. Previous investigations concerning PDAC gene expression profiling have diagnosed hundreds of DEGs.[13]

Bioinformatics analysis is a beneficial strategy for the broad analysis of large databases, including knotty genetic information. In our investigation, we used sophisticated bioinformatics methods to screen potential biomarkers that might be useful for PDAC. The Gene Expression Omnibus (GEO) (https://www.ncbi.nlm.nih.gov/geo/) database[14] is an open database that allows researchers to select appropriate NGS data. In our investigation, we obtained NGS data set from the GEO (GSE133684)[15] and searched for DEGs using limma package of R language. We then performed GO term and pathway enrichment analyses of the identified DEGs using the ToppGene database. Protein-protein interaction networks (PPIs) were constructed using Integrated Interactions Database (IID) interactome database and visualized using Cytoscape. Conduct module analyses of the PPI network were performed using PEWCC1. The associations of hub genes with PDAC were determined using a Kaplan-Meier analysis, expression analysis, stage analysis, mutation analysis, protein expression analysis, immune infiltration analysis, and receiver operating characteristic (ROC) curve analysis. Finally, PDAC-related genes were selected to investigate their potential role in a PDAC diagnostic, prognostic, and therapeutic target.

Materials and Methods

Next-generation sequencing data source

NGS data of human mRNA about PDAC research (GSE133684) were obtained from the GEO database The DEGs were considered by 1 independent PDAC data set, GSE133684[15] with 284 PDAC and 117 normal control samples. The GSE133684 NGS data were based on the GPL20795 HiSeq X Ten (*Homo sapiens*) platform..

Identification of DEGs

The limma package of R language was used for DEGs between PDAC and normal control samples.[16] The *P* value was adjusted by the Benjamini-Hochberg method.[17] An adjusted *P* value of <0.05 and $|\log2 \text{ fold change (FC)}| > 1$ were considered as threshold values for DEGs identification. The ggplot2 package and gplots package of R language were used to generate volcano plot and heat map. A volcano plot displays the logarithm of the *P* value on the y-axis and the logarithm of the fold-change between the 2 conditions on the x-axis. The *P*-value represents the statistical significance of the difference in gene expression between the 2 conditions, while the fold-change indicates the magnitude of the difference. Heat maps are particularly useful in gene expression analysis, where they are commonly used to visualize gene expression patterns across different experimental conditions or samples. The identified DEGs were preserved for further bioinformatics analysis.

GO analysis and pathway enrichment analysis of DEGs

The GO repository (http://geneontology.org/)[18] consists of a massive set of annotation terms and is generally used for annotating genes and identifying the distinctive biological aspects for NGS data. The REACTOME database (https://reactome.org/)[19] contains data on known genes and their biochemical functions and is used for identifying functional and metabolic pathways. By performing the GO and REACTOME enrichment analysis at the functional level, we can boost a better understanding of the roles of these DEGs in the induction and in the advancement of PDAC. The ToppGene (ToppFun) (https://toppgene.cchmc.org/enrichment.jsp)[20] is an online resource that adds tools for functional annotation and bioinformatics analysis. Both GO categories and REACTOME pathway enrichment analysis were implemented using ToppGene to inform the functions of these DEGs. $P < 0.05$ was considered to indicate a statistically significant difference.

PPI network construction and module analysis

The online database IID interactome (http://iid.ophid.utoronto.ca//)[21] was used to construct a PPI network of the proteins encoded by DEGs. Then, Cytoscape software (Version 3.8.1)[22] was applied to perform protein interaction association network analysis with confidence score > 0.4 and analyze the interaction correlation of the candidate proteins encoded by the DEGs in PDAC. Next, the Network Analyzer Cytoscape plug-in was applied to calculate node degree,[23] betweenness centrality,[24] stress centrality,[25] and closeness centrality.[26] Finally, the PEWCC1 (http://apps.cytoscape.org/apps/PEWCC1)[27] module for Cytoscape was used to collect the significant modules in the PPI network complex.

Construction of miRNA-DEG regulatory network

The miRNet database (https://www.mirnet.ca/)[28] is a database containing miRNAs involved in various diseases. The miRNAs related to PDAC were searched from miRNet database.

Through getting the intersection of the miRNAs and the DEGs, the miRNA-DEG regulatory relationships were selected. Finally, miRNA-DEG regulatory network was built using Cytoscape software.

Construction of TF-DEG regulatory network

The NetworkAnalyst database (https://www.networkanalyst.ca/)[29] is a database containing TFs involved in various diseases. The TFs related to PDAC were searched from TF database. Through getting the intersection of the TFs and the DEGs, the TF-DEG regulatory relationships were selected. Finally, TF-DEG regulatory network was built using Cytoscape software.

Validation of hub genes

After hub genes identified from expression profiling by high-throughput sequencing data set, UALCAN (http://ualcan.path.uab.edu/analysis.html)[30] was used to validate the selected upregulated and downregulated hub genes. UALCAN is an online tool for gene expression analysis between PDAC and normal data from the Cancer Genome Atlas (TCGA). It adds data such as gene expression, tumor staging, and survival period for PDAC. cBioPortal is an online platform (http://www.cbioportal.org)[31] for gene alteration of hub genes analysis from TCGA. Human protein atlas is an online database (HPA, www.proteinatlas.org)[32] for protein expression analysis between PDAC and normal data from TCGA. TIMER is an online platform (https://cistrome.shinyapps.io/timer/)[33] for immune infiltration analysis from TCGA. To explore diagnostic biomarkers of PDAC, we used the above hub genes as candidates to find their diagnostic value based on generalized linear model (GLM).[34] The pROC in R was used for receiver operating characteristic (ROC) curve analysis.[34] In brief, half of the samples (PDAC = 142, controls = 59) were aimlessly distributed as the training set and remaining data were used as the test set, which were used to set up a model. An ROC curve analysis was tested to calculate the specificity and sensitivity of the GLM prediction model. The area under the curve (AUC) was used to determine the diagnostic efficiency of the classifier.

Results

Identification of DEGs

We analyzed the DEGs of GSE133684 by using the limma package. We used $P < 0.05$ and $|\log FC| \geq 1$ as the cutoff criteria. We screened 463 DEGs, including 232 upregulated genes and 231 downregulated genes in PDAC samples compared with normal control samples, which are listed in Table 1. We identified all the DEGs that were shown in the above volcano map according to the value of |logFC| (shown in Figure 1) and then displayed the DEGs on a heatmap (shown in Figure 2).

GO analysis and pathway enrichment analysis of DEGs

To symbolize the function of the DEGs and to identify important candidate pathways, GO functional enrichment analysis and REACTOME pathway enrichment analysis were performed. The results of GO categories analysis, including biological processes (BP), cellular components (CC) and molecular functions (MF), are listed in Table 2. First, the upregulated genes were annotated with the BP category, including vesicle organization and secretion, whereas the downregulated genes were annotated with the GO terms, including lymphocyte activation and regulation of cell death. Second, the upregulated genes were annotated with the GO terms of the CC category, namely, secretory vesicle and whole membrane, whereas the downregulated genes were annotated with the GO terms, including cell surface and intrinsic component of plasma membrane. Third, the upregulated genes were annotated with the GO terms of the MF category such as protein dimerization activity and signaling receptor binding, whereas the downregulated genes were annotated with the GO terms, including transferase activity, transferring phosphorus-containing groups, and drug binding. The REACTOME pathway enrichment analysis showed that the genes upregulated in tumors were enriched in hemostasis and cell cycle, while the downregulated genes were enriched in adaptive immune system and transmembrane transport of small molecules (Table 3).

Protein–protein interaction (PPI) network construction and module analysis

After all the DEGs were uploaded to the online IID interactome database, the PPI network with 6188 nodes and 13153 edges was constructed using the Cytoscape software (Figure 3A). Hub genes with the node degree, betweenness centrality, stress centrality, and closeness centrality were obtained and are listed in Table 4. Cathepsin B (*CCNB1*) and four-and-a-half LIM domains 2 (*FHL2*) were the upregulated genes, while major histocompatibility complex, class II, DP alpha 1 (*HLA-DPA1*), and tubulin beta 1 class VI (*TUBB1*) were the downregulated genes. Then, 2 significant modules that fulfilled the cut-off criteria, namely, PEWCC1 scores > 3 and number of nodes > 5, were screened (Figure 3B and C). The fibrinogen beta chain (*FGB*), fibrinogen alpha chain (*FGA*), fibrinogen gamma chain (*FGG*), eukaryotic translation elongation factor 1 alpha 1 (*EEF1A1*), ribosomal protein L13a (*RPL13A*), integrin subunit alpha 4 (*ITGA4*), ribosomal protein L27a (*RPL27A*), ribosomal protein L23a (*RPL23A*), and ribosomal protein L10 (*RPL10*) genes were identified in these modules. GO analysis of these genes showed that they were annotated with vesicle organization, regulation of cell death, and lymphocyte activation. In addition, the REACTOME enrichment analysis suggested that these genes were mainly involved in hemostasis, innate immune system, and disease and adaptive immune system.

Table 1. The statistical metrics for key differentially expressed genes (DEGs).

GENE SYMBOL	LOGFC	P VALUE	ADJ.P.VAL	T VALUE	REGULATION	GENE NAME
DAP	0.729809	3.54E-14	2.59E-11	7.862623	Up	death associated protein
MTRNR2L2	1.55786	4.87E-14	3.22E-11	7.816552	Up	MT-RNR2 like 2
ICA1	1.027176	1.66E-13	9E-11	7.636838	Up	islet cell autoantigen 1
KRT8	1.61503	6.94E-13	3.01E-10	7.423576	Up	keratin 8
MAP1LC3B2	1.050642	1.03E-11	3.21E-09	7.008711	Up	microtubule associated protein 1 light chain 3 beta 2
KRT18	1.317775	1.21E-11	3.67E-09	6.984018	Up	keratin 18
DBN1	0.680188	1.71E-11	4.78E-09	6.928904	Up	drebrin 1
MAP1B	0.804673	2.02E-11	5.5E-09	6.902127	Up	microtubule associated protein 1B
IGFBP2	1.26743	2.04E-11	5.5E-09	6.900692	Up	insulin like growth factor binding protein 2
KRT19	1.682062	3.2E-11	8.32E-09	6.828975	Up	keratin 19
ARNTL2	1.064741	3.25E-11	8.42E-09	6.826429	Up	aryl hydrocarbon receptor nuclear translocator like 2
MND1	1.050388	6.48E-11	1.51E-08	6.714983	Up	meiotic nuclear divisions 1
LCN2	1.195504	1.23E-10	2.65E-08	6.610378	Up	lipocalin 2
HP	1.105468	1.98E-10	4.01E-08	6.531824	Up	haptoglobin
GOLIM4	0.730931	1.99E-10	4.01E-08	6.531295	Up	golgi integral membrane protein 4
FGB	1.281458	2.04E-10	4.09E-08	6.526862	Up	fibrinogen beta chain
TCEAL3	0.698058	2.11E-10	4.19E-08	6.521292	Up	transcription elongation factor A like 3
H3P47	0.806164	3.14E-10	5.88E-08	6.455108	Up	H3 histone pseudogene 47
CD27-AS1	1.127104	3.53E-10	6.52E-08	6.435648	Up	CD27 antisense RNA 1
LSMEM1	1.300595	3.94E-10	7.16E-08	6.417125	Up	leucine rich single-pass membrane protein 1
CD63	0.638758	4.97E-10	8.71E-08	6.378004	Up	CD63 molecule
MAOB	1.081308	7.82E-10	1.29E-07	6.301015	Up	monoamine oxidase B
FGG	1.037158	8.4E-10	1.36E-07	6.288927	Up	fibrinogen gamma chain
LOC105370027	1.046446	1.06E-09	1.66E-07	6.248715	Up	uncharacterized LOC105370027
H2BC17	0.973199	1.13E-09	1.75E-07	6.237457	Up	H2B clustered histone 17
ZFPM2	1.167509	1.26E-09	1.93E-07	6.218913	Up	zinc finger protein, FOG family member 2
UBE2Q2P1	0.75226	2.34E-09	3.3E-07	6.111953	Up	ubiquitin conjugating enzyme E2 Q2 pseudogene 1
GTF3C6	0.66658	2.41E-09	3.36E-07	6.107154	Up	general transcription factor IIIC subunit 6
FGA	1.058162	2.56E-09	3.52E-07	6.096366	Up	fibrinogen alpha chain
H4C15	0.646131	3.44E-09	4.5E-07	6.044383	Up	H4 clustered histone 15
TAX1BP3	0.761452	3.74E-09	4.85E-07	6.029641	Up	Tax1 binding protein 3
RET	0.748469	4.44E-09	5.62E-07	5.999495	Up	ret proto-oncogene
HTATIP2	0.696367	4.69E-09	5.87E-07	5.989713	Up	HIV-1 Tat interactive protein 2
MCEMP1	1.055887	7.5E-09	8.94E-07	5.906144	Up	mast cell expressed membrane protein 1
APOB	0.984349	8.66E-09	1.02E-06	5.88037	Up	apolipoprotein B
TPM2	0.808631	9.37E-09	1.09E-06	5.866037	Up	tropomyosin 2
MYL6B	0.735111	9.66E-09	1.12E-06	5.860685	Up	myosin light chain 6B
PRELID2	1.007003	1.01E-08	1.16E-06	5.851789	Up	PRELI domain containing 2
STAC	0.70663	1.08E-08	1.24E-06	5.839882	Up	SH3 and cysteine rich domain
H4C14	0.640786	1.16E-08	1.32E-06	5.826872	Up	H4 clustered histone 14
KLHDC8B	0.931058	1.17E-08	1.32E-06	5.825909	Up	kelch domain containing 8B
HRG	1.25373	1.49E-08	1.63E-06	5.782449	Up	histidine rich glycoprotein
DDAH1	0.960624	2.46E-08	2.46E-06	5.689878	Up	dimethylargininedimethylaminohydrolase 1
C19orf33	1.048033	2.73E-08	2.69E-06	5.670561	Up	chromosome 19 open reading frame 33
FAH	0.995091	3.02E-08	2.92E-06	5.651858	Up	fumarylacetoacetate hydrolase
DCBLD2	0.939546	3.06E-08	2.96E-06	5.649534	Up	discoidin, CUB and LCCL domain containing 2
IFI27L2	0.822377	3.76E-08	3.53E-06	5.611483	Up	interferon alpha inducible protein 27 like 2
PTGES3L	0.989667	3.95E-08	3.7E-06	5.602037	Up	prostaglandin E synthase 3 like
TIMP1	0.829195	4.17E-08	3.89E-06	5.591888	Up	TIMP metallopeptidase inhibitor 1
SNURF	0.743535	4.2E-08	3.91E-06	5.590685	Up	SNRPN upstream reading frame
CMTM2	0.918208	4.76E-08	4.36E-06	5.567227	Up	CKLF like MARVEL transmembrane domain containing 2
MDK	0.797135	6.31E-08	5.6E-06	5.513868	Up	midkine

(Continued)

Table 1. (Continued)

GENE SYMBOL	LOGFC	P VALUE	ADJ.P.VAL	T VALUE	REGULATION	GENE NAME
BCAP31	0.771229	6.77E-08	5.93E-06	5.500637	Up	B cell receptor associated protein 31
RAB32	0.725327	7.54E-08	6.49E-06	5.480174	Up	RAB32, member RAS oncogene family
PCP2	0.848727	7.79E-08	6.64E-06	5.474068	Up	Purkinje cell protein 2
AOPEP	0.665257	9.03E-08	7.61E-06	5.445854	Up	aminopeptidase O (putative)
FKBP1B	1.079675	9.08E-08	7.64E-06	5.444649	Up	FKBP prolylisomerase 1B
UBE2C	0.919203	9.19E-08	7.7E-06	5.442432	Up	ubiquitin conjugating enzyme E2 C
CETN2	0.907963	9.64E-08	7.99E-06	5.433373	Up	centrin 2
TREML3P	0.736245	1.04E-07	8.51E-06	5.418563	Up	triggering receptor expressed on myeloid cells like 3, pseudogene
CLMAT3	0.914772	1.09E-07	8.91E-06	5.409301	Up	colorectal liver metastasis associated transcript 3
TOM1L1	1.010788	1.25E-07	1E-05	5.382976	Up	target of myb1 like 1 membrane trafficking protein
RABAC1	0.685861	1.28E-07	1.02E-05	5.378165	Up	Rab acceptor 1
PTPRN	0.756419	1.8E-07	1.35E-05	5.312969	Up	protein tyrosine phosphatase receptor type N
CCDC9B	0.764226	1.89E-07	1.42E-05	5.302684	Up	coiled-coil domain containing 9B
UNC13B	0.669902	2.49E-07	1.8E-05	5.248667	Up	unc-13 homolog B
APOH	0.937929	2.62E-07	1.88E-05	5.238638	Up	apolipoprotein H
MCM10	0.778282	2.66E-07	1.9E-05	5.236183	Up	minichromosome maintenance 10 replication initiation factor
H2BC11	0.672283	2.8E-07	1.98E-05	5.226015	Up	H2B clustered histone 11
EZH2	0.665264	3E-07	2.1E-05	5.211928	Up	enhancer of zeste 2 polycomb repressive complex 2 subunit
H2AC13	0.672944	3.06E-07	2.14E-05	5.208195	Up	H2A clustered histone 13
NCBP2L	0.690397	3.18E-07	2.2E-05	5.200769	Up	nuclear cap binding protein subunit 2 like
CCNB1	0.69638	3.18E-07	2.2E-05	5.200386	Up	cyclin B1
PKD2	0.747713	3.28E-07	2.25E-05	5.194336	Up	polycystin 2, transient receptor potential cation channel
LOC100130357	0.908199	3.58E-07	2.43E-05	5.176869	Up	uncharacterized LOC100130357
ORM1	0.845653	4.18E-07	2.79E-05	5.145905	Up	orosomucoid 1
CDR2L	0.75789	4.37E-07	2.89E-05	5.137166	Up	cerebellar degeneration related protein 2 like
H2AJ	0.700133	4.63E-07	3.02E-05	5.125431	Up	H2A.J histone
TPM1	0.669813	4.65E-07	3.03E-05	5.124861	Up	tropomyosin 1
ACOT7	0.80117	5.34E-07	3.4E-05	5.097055	Up	acyl-CoA thioesterase 7
AP1M2	0.962099	5.68E-07	3.57E-05	5.084413	Up	adaptor related protein complex 1 subunit mu 2
AVEN	0.668545	6.52E-07	4.05E-05	5.056569	Up	apoptosis and caspase activation inhibitor
DNAH2	0.732007	6.75E-07	4.17E-05	5.049466	Up	dynein axonemal heavy chain 2
TRPC2	0.85544	7.09E-07	4.35E-05	5.039399	Up	transient receptor potential cation channel subfamily C member 2 (pseudogene)
RND3	0.841233	7.53E-07	4.58E-05	5.027115	Up	Rho family GTPase 3
PPP1R14A	0.745833	7.86E-07	4.75E-05	5.018397	Up	protein phosphatase 1 regulatory inhibitor subunit 14A
TGFB3	0.835809	7.9E-07	4.76E-05	5.01733	Up	transforming growth factor beta 3
TPST1	0.819069	8.34E-07	4.99E-05	5.006228	Up	tyrosylproteinsulfotransferase 1
VNN1	0.865209	1.1E-06	6.32E-05	4.949468	Up	vanin 1
MIR1282	1.063689	1.12E-06	6.41E-05	4.945828	Up	microRNA 1282
APOA2	0.724038	1.23E-06	6.93E-05	4.92633	Up	apolipoprotein A2
FAM92A	0.677465	1.25E-06	7.03E-05	4.922308	Up	family with sequence similarity 92 member A
MSANTD3	0.66954	1.29E-06	7.18E-05	4.916615	Up	Myb/SANT DNA binding domain containing 3
GRK4	0.900233	1.37E-06	7.55E-05	4.904444	Up	G protein-coupled receptor kinase 4
TSPAN15	0.802125	1.4E-06	7.7E-05	4.899117	Up	tetraspanin 15
PTGER3	0.731073	1.54E-06	8.36E-05	4.879106	Up	prostaglandin E receptor 3
MITF	0.871653	1.63E-06	8.76E-05	4.867297	Up	melanocyte inducing transcription factor
MMP1	0.771433	1.75E-06	9.33E-05	4.852725	Up	matrix metallopeptidase 1
MAL2	0.749667	1.81E-06	9.62E-05	4.845684	Up	mal, T cell differentiation protein 2 (gene/pseudogene)
CTPS2	0.67219	1.83E-06	9.71E-05	4.843038	Up	CTP synthase 2
LOC101929538	0.711706	1.9E-06	9.98E-05	4.835864	Up	uncharacterized LOC101929538
OR2B6	0.909758	1.94E-06	0.000102	4.831266	Up	olfactory receptor family 2 subfamily B member 6
C20orf96	0.740435	2.13E-06	0.000109	4.811175	Up	chromosome 20 open reading frame 96

(Continued)

Table 1. (Continued)

GENE SYMBOL	LOGFC	P VALUE	ADJ.P.VAL	T VALUE	REGULATION	GENE NAME
MPZL3	0.734878	2.16E-06	0.000111	4.808022	Up	myelin protein zero like 3
LOC101927420	0.734878	2.29E-06	0.000116	4.79601	Up	uncharacterized LOC101927420
EPDR1	0.769808	2.47E-06	0.000125	4.779781	Up	ependymin related 1
FHL2	0.853097	2.75E-06	0.000137	4.756748	Up	four and a half LIM domains 2
LAPTM4B	0.92193	3.02E-06	0.000148	4.736673	Up	lysosomal protein transmembrane 4 beta
ARG2	1.000424	3.03E-06	0.000149	4.735971	Up	arginase 2
ADAM22	0.710055	3.12E-06	0.000152	4.729888	Up	ADAM metallopeptidase domain 22
GPC5	0.6499	3.29E-06	0.000159	4.718778	Up	glypican 5
DERA	0.676038	3.31E-06	0.000161	4.716998	Up	deoxyribose-phosphate aldolase
OXTR	0.917126	3.55E-06	0.00017	4.70246	Up	oxytocin receptor
PROK2	0.789874	3.77E-06	0.000179	4.689155	Up	prokineticin 2
CNN1	0.901951	3.81E-06	0.00018	4.686924	Up	calponin 1
KRT7	0.904375	4.03E-06	0.000188	4.674982	Up	keratin 7
CENPI	0.730063	4.07E-06	0.00019	4.672762	Up	centromere protein I
LINC01684	0.731662	4.19E-06	0.000195	4.666397	Up	long intergenic non-protein coding RNA 1684
KCNMB1	0.752736	4.56E-06	0.000209	4.647801	Up	potassium calcium-activated channel subfamily M regulatory beta subunit 1
LACTB2	0.695963	4.69E-06	0.000215	4.641781	Up	lactamase beta 2
BEST3	0.711771	4.73E-06	0.000216	4.640144	Up	bestrophin 3
C5orf30	0.731538	5.21E-06	0.000236	4.618767	Up	chromosome 5 open reading frame 30
SMPD1	0.834518	5.41E-06	0.000244	4.610568	Up	sphingomyelinphosphodiesterase 1
ANO10	0.657575	5.46E-06	0.000246	4.608531	Up	anoctamin 10
GINS1	0.706019	5.61E-06	0.000252	4.602785	Up	GINS complex subunit 1
TGFB1I1	0.782636	6.07E-06	0.000269	4.585606	Up	transforming growth factor beta 1 induced transcript 1
CABLES1	0.659259	6.29E-06	0.000277	4.577514	Up	Cdk5 and Abl enzyme substrate 1
ROBO1	0.71818	7.03E-06	0.000304	4.552913	Up	roundabout guidance receptor 1
BUB1	0.667318	7.42E-06	0.000319	4.541048	Up	BUB1 mitotic checkpoint serine/threonine kinase
FUNDC1	0.767386	7.66E-06	0.000328	4.533938	Up	FUN14 domain containing 1
CRTC3-AS1	0.751802	7.83E-06	0.000334	4.529039	Up	CRTC3 antisense RNA 1
DMC1	0.841001	7.84E-06	0.000334	4.528894	Up	DNA meiotic recombinase 1
ZSCAN16-AS1	0.738009	8.09E-06	0.000344	4.521862	Up	ZSCAN16 antisense RNA 1
SCARF1	0.676906	8.39E-06	0.000355	4.513776	Up	scavenger receptor class F member 1
ACCSL	0.65649	8.65E-06	0.000365	4.50688	Up	1-aminocyclopropane-1-carboxylate synthase homolog (inactive) like
CXCL3	0.778559	1.03E-05	0.000421	4.468754	Up	C-X-C motif chemokine ligand 3
LINC00892	0.819555	1.05E-05	0.00043	4.462734	Up	long intergenic non-protein coding RNA 892
RNF208	0.841349	1.06E-05	0.000433	4.461088	Up	ring finger protein 208
EAF2	0.668192	1.15E-05	0.000464	4.443023	Up	ELL associated factor 2
LAMB2	0.699363	1.16E-05	0.000468	4.44064	Up	laminin subunit beta 2
LOXL3	0.736971	1.19E-05	0.000477	4.435804	Up	lysyl oxidase like 3
CEACAM6	0.828845	1.22E-05	0.000489	4.429132	Up	CEA cell adhesion molecule 6
HPD	0.801889	1.29E-05	0.00051	4.417691	Up	4-hydroxyphenylpyruvate dioxygenase
TMEM67	0.706644	1.3E-05	0.000511	4.415933	Up	transmembrane protein 67
LINC00534	0.991484	1.3E-05	0.000511	4.415737	Up	long intergenic non-protein coding RNA 534
TYMS	0.660517	1.31E-05	0.000514	4.413975	Up	thymidylatesynthetase
ZGLP1	0.781496	1.36E-05	0.000529	4.405803	Up	zinc finger GATA like protein 1
GNG8	0.74057	1.51E-05	0.000581	4.381524	Up	G protein subunit gamma 8
MT1X	0.78313	1.59E-05	0.000609	4.368771	Up	metallothionein 1X
EVA1B	0.700855	1.71E-05	0.000642	4.352699	Up	eva-1 homolog B
FRMD3	0.658149	1.91E-05	0.000704	4.326801	Up	FERM domain containing 3
ADAMTS1	0.710457	1.94E-05	0.000709	4.324203	Up	ADAM metallopeptidase with thrombospondin type 1 motif 1
ACTR3B	0.733415	2.06E-05	0.00075	4.309603	Up	actin related protein 3B
METTL22	0.69995	2.27E-05	0.00082	4.286931	Up	methyltransferase like 22

(Continued)

Table 1. (Continued)

GENE SYMBOL	LOGFC	P VALUE	ADJ.P.VAL	T VALUE	REGULATION	GENE NAME
WASF1	0.742178	2.34E-05	0.000842	4.280128	Up	WASP family member 1
LINC00548	0.776323	2.51E-05	0.000886	4.264099	Up	long intergenic non-protein coding RNA 548
DTL	0.641962	2.52E-05	0.00089	4.262623	Up	denticleless E3 ubiquitin protein ligase homolog
NT5DC2	0.692809	2.71E-05	0.000939	4.245871	Up	5'-nucleotidase domain containing 2
VEGFC	0.669813	2.88E-05	0.000989	4.231356	Up	vascular endothelial growth factor C
MAGI2	0.735314	2.89E-05	0.00099	4.230904	Up	membrane associated guanylate kinase, WW and PDZ domain containing 2
LINC00211	0.894161	2.93E-05	0.001001	4.227722	Up	long intergenic non-protein coding RNA 211
SPHK1	0.676802	3.04E-05	0.001028	4.219226	Up	sphingosine kinase 1
ZNF529-AS1	0.661567	3.35E-05	0.001114	4.196168	Up	ZNF529 antisense RNA 1
ADAMTS5	0.660099	3.39E-05	0.001123	4.193506	Up	ADAM metallopeptidase with thrombospondin type 1 motif 5
DYNC1I1	0.795012	3.39E-05	0.001124	4.193181	Up	dynein cytoplasmic 1 intermediate chain 1
CCDC3	0.674572	3.42E-05	0.001131	4.191397	Up	coiled-coil domain containing 3
YIF1B	0.743761	3.43E-05	0.001133	4.190185	Up	Yip1 interacting factor homolog B, membrane trafficking protein
PRKAR1B	0.701104	3.54E-05	0.001164	4.182731	Up	protein kinase cAMP-dependent type I regulatory subunit beta
NMNAT3	0.641441	4.03E-05	0.001305	4.151903	Up	nicotinamide nucleotide adenylyltransferase 3
TSPAN13	0.656865	4.05E-05	0.00131	4.150707	Up	tetraspanin 13
POLR3G	0.862253	4.19E-05	0.001346	4.143028	Up	RNA polymerase III subunit G
TMEM158	0.832551	4.39E-05	0.0014	4.131626	Up	transmembrane protein 158 (gene/pseudogene)
CYTOR	0.669042	4.41E-05	0.001403	4.130782	Up	cytoskeleton regulator RNA
FN3K	0.715739	4.44E-05	0.001411	4.128739	Up	fructosamine 3 kinase
CENPU	0.685833	4.48E-05	0.001421	4.126825	Up	centromere protein U
ANXA3	0.642891	4.52E-05	0.001431	4.124872	Up	annexin A3
PGLYRP1	0.743358	4.53E-05	0.001432	4.124178	Up	peptidoglycan recognition protein 1
LINC00853	0.886342	4.73E-05	0.001482	4.113907	Up	long intergenic non-protein coding RNA 853
C21orf58	0.673046	5E-05	0.001552	4.10054	Up	chromosome 21 open reading frame 58
PHACTR3	0.768701	5.12E-05	0.001582	4.094798	Up	phosphatase and actin regulator 3
CYSTM1	0.639491	6.02E-05	0.001809	4.055347	Up	cysteine rich transmembrane module containing 1
E2F1	0.689528	6.28E-05	0.001867	4.045197	Up	E2F transcription factor 1
CTNS	0.723506	6.31E-05	0.001876	4.043771	Up	cystinosin, lysosomalcystine transporter
LUZP6	0.784849	6.33E-05	0.00188	4.043183	Up	leucine zipper protein 6
LY6G6F-LY6G6D	0.697512	6.82E-05	0.002	4.024994	Up	LY6G6F-LY6G6D readthrough
DRC7	0.641026	6.97E-05	0.00203	4.019452	Up	dynein regulatory complex subunit 7
SPINT2	0.716213	7.44E-05	0.002142	4.003447	Up	serine peptidase inhibitor, Kunitz type 2
TST	0.653129	8.57E-05	0.002428	3.968702	Up	thiosulfate sulfurtransferase
PBLD	0.728909	9.82E-05	0.002708	3.934854	Up	phenazine biosynthesis like protein domain containing
COL6A3	0.800552	0.000106	0.002866	3.916014	Up	collagen type VI alpha 3 chain
SMYD3	0.658545	0.00011	0.002954	3.906774	Up	SET and MYND domain containing 3
SEPTIN4	0.678613	0.000113	0.003014	3.900217	Up	septin 4
ADAM32	0.660263	0.000114	0.003032	3.898284	Up	ADAM metallopeptidase domain 32
ADH1B	0.683312	0.000115	0.003044	3.896241	Up	alcohol dehydrogenase 1B (class I), beta polypeptide
TTLL7	0.772356	0.000116	0.003081	3.892908	Up	tubulin tyrosine ligase like 7
ME1	0.679181	0.000119	0.003134	3.887332	Up	malic enzyme 1
PADI4	0.638723	0.000119	0.00315	3.885738	Up	peptidyl arginine deiminase 4
CIDECP1	0.65588	0.000123	0.003226	3.877866	Up	cell death inducing DFFA like effector c pseudogene 1
CD151	0.680244	0.000133	0.003439	3.859108	Up	CD151 molecule (Raph blood group)
ETV4	0.762875	0.000137	0.003518	3.851736	Up	ETS variant transcription factor 4
MYOM1	0.712787	0.000141	0.003611	3.843573	Up	myomesin 1
MSANTD3-TMEFF1	0.694055	0.000161	0.00403	3.810035	Up	MSANTD3-TMEFF1 readthrough
GLA	0.768164	0.000169	0.004193	3.797347	Up	galactosidase alpha
TRHDE	0.673175	0.000173	0.004275	3.791127	Up	thyrotropin releasing hormone degrading enzyme
CCT6P3	0.64622	0.000176	0.00433	3.786849	Up	chaperonin containing TCP1 subunit 6 pseudogene 3
DNAH14	0.67538	0.000197	0.004737	3.757991	Up	dynein axonemal heavy chain 14

(Continued)

Table 1. (Continued)

GENE SYMBOL	LOGFC	P VALUE	ADJ.P.VAL	T VALUE	REGULATION	GENE NAME
PLEKHA8P1	0.678922	0.000198	0.004758	3.756381	Up	pleckstrin homology domain containing A8 pseudogene 1
MIR646HG	0.725938	0.0002	0.004796	3.753511	Up	MIR646 host gene
TMEFF1	0.71416	0.000213	0.005026	3.73756	Up	transmembrane protein with EGF like and two follistatin like domains 1
DPY19L2	0.678632	0.000214	0.005044	3.736377	Up	dpy-19 like 2
ERC2	0.640215	0.000232	0.005396	3.715528	Up	ELKS/RAB6-interacting/CAST family member 2
PLA2G4A	0.672732	0.000232	0.005396	3.715504	Up	phospholipase A2 group IVA
ZC3HAV1L	0.67853	0.000241	0.005556	3.705049	Up	zinc finger CCCH-type containing, antiviral 1 like
AQP10	0.702387	0.000255	0.005825	3.690433	Up	aquaporin 10
PRTFDC1	0.732046	0.000266	0.006032	3.67956	Up	phosphoribosyltransferase domain containing 1
SERPINE2	0.708281	0.000278	0.006263	3.667198	Up	serpin family E member 2
PRR16	0.647548	0.000365	0.007821	3.594668	Up	proline rich 16
ACER2	0.714054	0.000441	0.009068	3.543878	Up	alkaline ceramidase 2
THEM5	0.68475	0.000632	0.012136	3.44491	Up	thioesterase superfamily member 5
MS4A3	0.669703	0.000713	0.013422	3.41125	Up	membrane spanning 4-domains A3
CLEC2L	0.667059	0.000745	0.013903	3.398829	Up	C-type lectin domain family 2 member L
TRPC6	0.669122	0.000816	0.014941	3.373194	Up	transient receptor potential cation channel subfamily C member 6
LINC01089	0.641558	0.00098	0.017284	3.320844	Up	long intergenic non-protein coding RNA 1089
GRB14	0.73252	0.001457	0.023689	3.205476	Up	growth factor receptor bound protein 14
MYEOV	0.66784	0.001553	0.024891	3.186553	Up	myeloma overexpressed
TNNC2	0.681795	0.001798	0.027848	3.142855	Up	troponin C2, fast skeletal type
PLAAT1	0.716924	0.001991	0.030092	3.112202	Up	phospholipase A and acyltransferase 1
INKA2-AS1	0.64851	0.002272	0.033302	3.072049	Up	INKA2 antisense RNA 1
DEFA1	0.710406	0.002482	0.035699	3.044927	Up	defensin alpha 1
LYPLAL1-DT	0.653678	0.00251	0.035991	3.041436	Up	LYPLAL1 divergent transcript
G0S2	0.666254	0.003148	0.04269	2.970966	Up	G0/G1 switch 2
LOC105371967	0.715866	0.00336	0.044907	2.950485	Up	uncharacterized LOC105371967
FBXO7	-1.02578	4.57E-31	2.47E-26	-12.6471	Down	F-box protein 7
CD44	-0.77354	1.37E-24	3.7E-20	-10.9533	Down	CD44 molecule (Indian blood group)
BNIP3L	-1.11652	7.58E-24	1.37E-19	-10.7506	Down	BCL2 interacting protein 3 like
ITGA4	-0.7155	7.16E-22	6.46E-18	-10.202	Down	integrin subunit alpha 4
SRRM2	-0.7545	2.82E-21	1.74E-17	-10.0332	Down	serine/arginine repetitive matrix 2
IL7R	-0.9167	3.22E-21	1.74E-17	-10.0169	Down	interleukin 7 receptor
HLA-DRA	-0.72512	6.41E-21	2.89E-17	-9.93149	Down	major histocompatibility complex, class II, DR alpha
AHNAK	-1.08285	1.37E-20	5.71E-17	-9.83691	Down	AHNAK nucleoprotein
SESN3	-0.83384	3.7E-20	1.34E-16	-9.71209	Down	sestrin 3
BTG1	-0.67464	8.57E-20	2.9E-16	-9.606	Down	BTG anti-proliferation factor 1
TCF7	-1.05537	9.82E-20	3.13E-16	-9.58878	Down	transcription factor 7
PTPRC	-0.79038	1.95E-19	5.55E-16	-9.50153	Down	protein tyrosine phosphatase receptor type C
STK17B	-0.6627	8.27E-19	1.95E-15	-9.31582	Down	serine/threonine kinase 17b
IKZF3	-0.84512	4.27E-18	9.64E-15	-9.10211	Down	IKAROS family zinc finger 3
OGT	-0.85075	8.43E-18	1.83E-14	-9.01274	Down	O-linked N-acetylglucosamine (GlcNAc) transferase
MALAT1	-1.15502	1.98E-17	4.04E-14	-8.89988	Down	metastasis associated lung adenocarcinoma transcript 1
MBNL3	-0.85006	2.01E-17	4.04E-14	-8.89733	Down	muscleblind like splicing regulator 3
TXNIP	-0.69647	3.04E-17	5.67E-14	-8.8425	Down	thioredoxin interacting protein
SLC38A1	-0.674	7.23E-17	1.22E-13	-8.72615	Down	solute carrier family 38 member 1
NCKAP1L	-0.66777	7.45E-17	1.22E-13	-8.72221	Down	NCK associated protein 1 like
PAX5	-1.15676	2.44E-16	3.67E-13	-8.56139	Down	paired box 5
TNRC6B	-0.80631	3.35E-16	4.86E-13	-8.51801	Down	trinucleotide repeat containing adaptor 6B
ATM	-0.65967	4.2E-16	5.83E-13	-8.48699	Down	ATM serine/threonine kinase
HLA-DPA1	-0.67781	1.41E-15	1.82E-12	-8.31961	Down	major histocompatibility complex, class II, DP alpha 1
FAM102A	-0.76298	1.5E-15	1.89E-12	-8.31093	Down	family with sequence similarity 102 member A

(Continued)

Table 1. (Continued)

GENE SYMBOL	LOGFC	P VALUE	ADJ.P.VAL	T VALUE	REGULATION	GENE NAME
DYRK2	-0.69741	1.54E-15	1.89E-12	-8.30769	Down	dual specificity tyrosine phosphorylation regulated kinase 2
STRADB	-0.88854	2.32E-15	2.7E-12	-8.24996	Down	STE20 related adaptor beta
RNF213	-0.78696	2.36E-15	2.7E-12	-8.2476	Down	ring finger protein 213
RPL10	-0.68279	2.4E-15	2.7E-12	-8.24564	Down	ribosomal protein L10
EEF1A1	-0.93399	4.56E-15	4.75E-12	-8.15527	Down	eukaryotic translation elongation factor 1 alpha 1
RPL23A	-0.69095	5.13E-15	5.14E-12	-8.13875	Down	ribosomal protein L23a
RPL37	-0.68343	6.21E-15	5.9E-12	-8.11176	Down	ribosomal protein L37
HBB	-1.18457	1.01E-14	9.1E-12	-8.04285	Down	hemoglobin subunit beta
CAMK4	-1.1638	1.36E-14	1.17E-11	-8.00017	Down	calcium/calmodulin dependent protein kinase IV
TENT5C	-0.78619	1.47E-14	1.24E-11	-7.98892	Down	terminal nucleotidyltransferase 5C
BACH2	-1.06422	1.5E-14	1.24E-11	-7.98579	Down	BTB domain and CNC homolog 2
TBCEL	-0.64594	1.51E-14	1.24E-11	-7.98482	Down	tubulin folding cofactor E like
WDFY4	-0.99635	2.23E-14	1.75E-11	-7.9292	Down	WDFY family member 4
RPL27A	-0.6388	2.37E-14	1.83E-11	-7.92052	Down	ribosomal protein L27a
AAK1	-0.65765	4.11E-14	2.89E-11	-7.8413	Down	AP2 associated kinase 1
MS4A1	-0.95361	4.31E-14	2.96E-11	-7.8342	Down	membrane spanning 4-domains A1
DCAF12	-0.7593	5.05E-14	3.3E-11	-7.81122	Down	DDB1 and CUL4 associated factor 12
KMT2D	-0.87707	5.94E-14	3.83E-11	-7.78757	Down	lysine methyltransferase 2D
OPA1	-0.62121	6.75E-14	4.3E-11	-7.76907	Down	OPA1 mitochondrial dynamin like GTPase
CAMK1D	-0.67422	1.2E-13	6.98E-11	-7.68504	Down	calcium/calmodulin dependent protein kinase ID
FAM117B	-0.73486	1.2E-13	6.98E-11	-7.68502	Down	family with sequence similarity 117 member B
BCL11B	-0.71547	1.26E-13	7.28E-11	-7.67723	Down	BAF chromatin remodeling complex subunit BCL11B
HBA1	-1.28343	1.39E-13	7.86E-11	-7.66283	Down	hemoglobin subunit alpha 1
SEC16A	-0.63051	2.06E-13	1.07E-10	-7.60474	Down	SEC16 homolog A, endoplasmic reticulum export factor
NOTCH2	-1.02848	3.2E-13	1.62E-10	-7.53985	Down	notch receptor 2
SLC25A37	-0.97321	3.22E-13	1.62E-10	-7.53857	Down	solute carrier family 25 member 37
BCL9L	-0.7821	3.41E-13	1.67E-10	-7.53032	Down	BCL9 like
RCAN3	-0.67723	3.62E-13	1.75E-10	-7.52118	Down	RCAN family member 3
RALGPS2	-0.81589	4.58E-13	2.08E-10	-7.48622	Down	Ral GEF with PH domain and SH3 binding motif 2
SOX6	-1.09995	5.44E-13	2.43E-10	-7.46032	Down	SRY-box transcription factor 6
TRANK1	-0.70118	6.86E-13	2.99E-10	-7.4255	Down	tetratricopeptide repeat and ankyrin repeat containing 1
IL10RA	-0.80857	7.25E-13	3.11E-10	-7.41713	Down	interleukin 10 receptor subunit alpha
TCP11L2	-0.85596	8.16E-13	3.42E-10	-7.39924	Down	t-complex 11 like 2
TMC8	-0.90771	8.95E-13	3.69E-10	-7.38532	Down	transmembrane channel like 8
HBA2	-1.1918	1.49E-12	5.84E-10	-7.30802	Down	hemoglobin subunit alpha 2
ZBTB20	-0.68652	2.37E-12	8.9E-10	-7.23703	Down	zinc finger and BTB domain containing 20
CTSB	-0.68749	3.44E-12	1.27E-09	-7.17953	Down	cathepsin B
NSUN3	-0.97469	3.57E-12	1.3E-09	-7.17397	Down	NOP2/Sun RNA methyltransferase 3
MARCHF8	-0.64518	4.02E-12	1.45E-09	-7.15528	Down	membrane associated ring-CH-type finger 8
BLK	-0.93113	4.45E-12	1.6E-09	-7.13963	Down	BLK proto-oncogene, Src family tyrosine kinase
LEF1	-0.72094	5.64E-12	1.97E-09	-7.10302	Down	lymphoid enhancer binding factor 1
TLCD4	-0.94983	5.98E-12	2.04E-09	-7.09373	Down	TLC domain containing 4
CBLB	-0.62042	6.13E-12	2.06E-09	-7.08996	Down	Cbl proto-oncogene B
IFIT1B	-1.14286	7.54E-12	2.43E-09	-7.05769	Down	interferon induced protein with tetratricopeptide repeats 1B
NLRP1	-0.70059	8.94E-12	2.81E-09	-7.03094	Down	NLR family pyrin domain containing 1
SORL1	-0.74274	1.46E-11	4.32E-09	-6.95383	Down	sortilin related receptor 1
IGF2R	-0.81797	1.48E-11	4.34E-09	-6.95175	Down	insulin like growth factor 2 receptor
PLEC	-0.76357	1.63E-11	4.68E-09	-6.93634	Down	plectin
EEF2	-0.65473	1.63E-11	4.68E-09	-6.93587	Down	eukaryotic translation elongation factor 2
AFF3	-0.87612	1.65E-11	4.71E-09	-6.93416	Down	AF4/FMR2 family member 3
YOD1	-0.88888	1.72E-11	4.78E-09	-6.92773	Down	YOD1 deubiquitinase
SFT2D2	-0.63701	2E-11	5.49E-09	-6.90414	Down	SFT2 domain containing 2

(Continued)

Table 1. (Continued)

GENE SYMBOL	LOGFC	P VALUE	ADJ.P.VAL	T VALUE	REGULATION	GENE NAME
NIBAN3	-0.99082	2.03E-11	5.5E-09	-6.90116	Down	niban apoptosis regulator 3
POU2F2	-0.62862	2.43E-11	6.49E-09	-6.87264	Down	POU class 2 homeobox 2
BCL11A	-0.69858	3.3E-11	8.52E-09	-6.82374	Down	BAF chromatin remodeling complex subunit BCL11A
CLEC17A	-0.81849	3.72E-11	9.42E-09	-6.80453	Down	C-type lectin domain containing 17A
ARL4A	-0.79887	3.94E-11	9.88E-09	-6.79545	Down	ADP ribosylation factor like GTPase 4A
TLCD4-RWDD3	-0.96826	4.03E-11	1E-08	-6.79186	Down	TLCD4-RWDD3 readthrough
SCARNA21B	-1.42152	4.37E-11	1.07E-08	-6.77868	Down	small Cajal body-specific RNA 21B
RANBP10	-0.73457	5.18E-11	1.22E-08	-6.75141	Down	RAN binding protein 10
BMF	-0.79975	6.24E-11	1.46E-08	-6.72111	Down	Bcl2 modifying factor
CLEC2D	-0.68117	9.34E-11	2.09E-08	-6.65559	Down	C-type lectin domain family 2 member D
CIITA	-0.75359	1.01E-10	2.25E-08	-6.64292	Down	class II major histocompatibility complex transactivator
TTN	-1.14193	1.17E-10	2.57E-08	-6.61882	Down	titin
SLC4A1	-1.02319	1.56E-10	3.25E-08	-6.57166	Down	solute carrier family 4 member 1 (Diego blood group)
VSTM2A	-0.78114	1.64E-10	3.41E-08	-6.56331	Down	V-set and transmembrane domain containing 2A
FGL2	-0.65079	1.81E-10	3.71E-08	-6.54693	Down	fibrinogen like 2
RORA	-0.65858	1.96E-10	3.99E-08	-6.53369	Down	RAR related orphan receptor A
TNFRSF13C	-0.91687	2.97E-10	5.64E-08	-6.46456	Down	TNF receptor superfamily member 13C
EP400	-0.66759	3.19E-10	5.96E-08	-6.45231	Down	E1A binding protein p400
PER1	-0.85447	3.87E-10	7.05E-08	-6.42021	Down	period circadian regulator 1
MPEG1	-0.67212	5.39E-10	9.42E-08	-6.3641	Down	macrophage expressed 1
MGAT4A	-0.65772	5.49E-10	9.55E-08	-6.36127	Down	alpha-1,3-mannosyl-glycoprotein 4-beta-N-acetylglucosaminyltransferase A
OSBPL10	-0.76921	6.1E-10	1.04E-07	-6.34334	Down	oxysterol binding protein like 10
SLC2A1	-1.01788	6.65E-10	1.13E-07	-6.32861	Down	solute carrier family 2 member 1
PLAGL2	-0.65128	7.62E-10	1.27E-07	-6.30558	Down	PLAG1 like zinc finger 2
WDFY2	-0.69295	7.76E-10	1.29E-07	-6.30233	Down	WD repeat and FYVE domain containing 2
SLC14A1	-0.82792	7.81E-10	1.29E-07	-6.30132	Down	solute carrier family 14 member 1 (Kidd blood group)
VIPR1	-0.76825	8.51E-10	1.37E-07	-6.28656	Down	vasoactive intestinal peptide receptor 1
TFRC	-0.80086	8.7E-10	1.39E-07	-6.28281	Down	transferrin receptor
AGPAT4	-0.83329	9.33E-10	1.48E-07	-6.27089	Down	1-acylglycerol-3-phosphate O-acyltransferase 4
COBLL1	-0.72259	1.01E-09	1.59E-07	-6.25677	Down	cordon-bleu WH2 repeat protein like 1
SPOCK2	-0.89285	1.11E-09	1.74E-07	-6.24084	Down	SPARC (osteonectin), cwcv and kazal like domains proteoglycan 2
FECH	-0.79692	1.35E-09	2.03E-07	-6.20743	Down	ferrochelatase
HLA-DMB	-0.71841	1.47E-09	2.19E-07	-6.19232	Down	major histocompatibility complex, class II, DM beta
MXI1	-0.66288	1.67E-09	2.43E-07	-6.17102	Down	MAX interactor 1, dimerization protein
TRAK2	-0.99989	1.9E-09	2.73E-07	-6.14798	Down	trafficking kinesin protein 2
TSPAN5	-0.68028	3.29E-09	4.34E-07	-6.05219	Down	tetraspanin 5
SPTA1	-1.01751	4.06E-09	5.21E-07	-6.01532	Down	spectrin alpha, erythrocytic 1
SCARNA10	-1.16787	4.37E-09	5.55E-07	-6.00252	Down	small Cajal body-specific RNA 10
CXCR5	-0.91719	5.95E-09	7.25E-07	-5.9476	Down	C-X-C motif chemokine receptor 5
KLK1	-0.94232	6.66E-09	8.03E-07	-5.92739	Down	kallikrein 1
CTC1	-0.70188	8.37E-09	9.87E-07	-5.88644	Down	CST telomere replication complex component 1
ALDH5A1	-0.71117	9.58E-09	1.11E-06	-5.86216	Down	aldehyde dehydrogenase 5 family member A1
YIPF4	-0.68858	9.91E-09	1.14E-06	-5.85599	Down	Yip1 domain family member 4
SZT2	-0.73017	1.03E-08	1.18E-06	-5.84867	Down	SZT2 subunit of KICSTOR complex
MIAT	-0.63403	1.18E-08	1.33E-06	-5.82457	Down	myocardial infarction associated transcript
LENG8	-0.63693	1.58E-08	1.72E-06	-5.7713	Down	leukocyte receptor cluster member 8
SLC7A6	-0.77445	1.83E-08	1.94E-06	-5.74413	Down	solute carrier family 7 member 6
PLBD2	-0.83269	1.94E-08	2.05E-06	-5.73332	Down	phospholipase B domain containing 2
RPL13A	-0.62991	2.15E-08	2.21E-06	-5.71499	Down	ribosomal protein L13a
TNFRSF13B	-0.94543	2.39E-08	2.41E-06	-5.6953	Down	TNF receptor superfamily member 13B
CD22	-0.67168	2.5E-08	2.49E-06	-5.68696	Down	CD22 molecule

(Continued)

Table 1. (Continued)

GENE SYMBOL	LOGFC	P VALUE	ADJ.P.VAL	T VALUE	REGULATION	GENE NAME
SERINC5	-0.73923	2.52E-08	2.5E-06	-5.6859	Down	serine incorporator 5
GPRASP1	-0.81967	2.57E-08	2.55E-06	-5.68227	Down	G protein-coupled receptor associated sorting protein 1
ADA2	-0.73878	2.61E-08	2.58E-06	-5.67885	Down	adenosine deaminase 2
CCR7	-0.82793	2.73E-08	2.68E-06	-5.67111	Down	C-C motif chemokine receptor 7
SCARNA6	-0.77803	2.88E-08	2.81E-06	-5.66069	Down	small Cajal body-specific RNA 6
CNKSR2	-0.75294	3.18E-08	3.06E-06	-5.64253	Down	connector enhancer of kinase suppressor of Ras 2
VCAN	-0.73858	3.74E-08	3.52E-06	-5.61242	Down	versican
SLC24A4	-0.87802	4.35E-08	4.03E-06	-5.58396	Down	solute carrier family 24 member 4
LINC00926	-0.87511	4.52E-08	4.17E-06	-5.57692	Down	long intergenic non-protein coding RNA 926
ACSL6	-0.82878	4.81E-08	4.39E-06	-5.56537	Down	acyl-CoA synthetase long chain family member 6
TTC14	-0.89136	4.84E-08	4.41E-06	-5.5642	Down	tetratricopeptide repeat domain 14
FCRL1	-0.86187	5.34E-08	4.82E-06	-5.54543	Down	Fc receptor like 1
SLC25A39	-0.68018	5.46E-08	4.91E-06	-5.54135	Down	solute carrier family 25 member 39
LY9	-0.76456	5.66E-08	5.08E-06	-5.53456	Down	lymphocyte antigen 9
GOLGA8A	-0.83441	7.01E-08	6.08E-06	-5.49414	Down	golgin A8 family member A
ATP2B1	-0.62628	7.37E-08	6.37E-06	-5.48451	Down	ATPase plasma membrane Ca2+ transporting 1
PWAR5	-0.75691	8.03E-08	6.79E-06	-5.46817	Down	PraderWilli/Angelman region RNA 5
MRC2	-0.81976	9.06E-08	7.63E-06	-5.44524	Down	mannose receptor C type 2
SPIB	-0.63152	9.37E-08	7.82E-06	-5.43865	Down	Spi-B transcription factor
GRINA	-0.65332	1.01E-07	8.28E-06	-5.42515	Down	glutamate ionotropic receptor NMDA type subunit associated protein 1
LRP1	-0.84115	1.01E-07	8.28E-06	-5.42512	Down	LDL receptor related protein 1
ADAM28	-0.81306	1.11E-07	9.02E-06	-5.40656	Down	ADAM metallopeptidase domain 28
TRABD2A	-0.7573	1.16E-07	9.42E-06	-5.39715	Down	TraB domain containing 2A
PIEZO1	-0.74385	1.17E-07	9.44E-06	-5.39644	Down	piezo type mechanosensitive ion channel component 1
ADAM19	-0.68425	1.47E-07	1.15E-05	-5.35189	Down	ADAM metallopeptidase domain 19
PARP15	-0.71333	2.02E-07	1.5E-05	-5.29026	Down	poly(ADP-ribose) polymerase family member 15
CD27	-0.71993	2.07E-07	1.53E-05	-5.28562	Down	CD27 molecule
NELL2	-0.67846	2.21E-07	1.62E-05	-5.27231	Down	neural EGFL like 2
CD79A	-0.74535	2.38E-07	1.73E-05	-5.2578	Down	CD79a molecule
ANKRD52	-0.63287	2.6E-07	1.87E-05	-5.24037	Down	ankyrin repeat domain 52
DNHD1	-0.7211	2.8E-07	1.98E-05	-5.22571	Down	dynein heavy chain domain 1
NEURL1	-0.74572	2.93E-07	2.06E-05	-5.21673	Down	neuralized E3 ubiquitin protein ligase 1
CRTC1	-0.68306	3.27E-07	2.25E-05	-5.1949	Down	CREB regulated transcription coactivator 1
GOLGA8B	-0.84973	3.8E-07	2.56E-05	-5.16529	Down	golgin A8 family member B
ZNF860	-0.72407	3.83E-07	2.58E-05	-5.16356	Down	zinc finger protein 860
P2RX5	-0.67155	3.84E-07	2.58E-05	-5.16328	Down	purinergic receptor P2X 5
BTLA	-0.73832	3.96E-07	2.65E-05	-5.15708	Down	B and T lymphocyte associated
OBSCN	-0.80054	4.42E-07	2.91E-05	-5.13505	Down	obscurin, cytoskeletal calmodulin and titin-interacting RhoGEF
SEMA7A	-0.6976	4.47E-07	2.94E-05	-5.13259	Down	semaphorin 7A (John Milton Hagen blood group)
IFFO1	-0.65589	4.96E-07	3.2E-05	-5.11184	Down	intermediate filament family orphan 1
SLC38A5	-0.75551	5.64E-07	3.56E-05	-5.0858	Down	solute carrier family 38 member 5
LINC02273	-0.70556	5.67E-07	3.57E-05	-5.08477	Down	long intergenic non-protein coding RNA 2273
DNAH1	-0.7411	6.47E-07	4.02E-05	-5.05819	Down	dynein axonemal heavy chain 1
NEU3	-0.70715	7.2E-07	4.4E-05	-5.03638	Down	neuraminidase 3
POLM	-0.67693	7.44E-07	4.53E-05	-5.02954	Down	DNA polymerase mu
RPS6KA5	-0.67198	8.28E-07	4.96E-05	-5.00771	Down	ribosomal protein S6 kinase A5
PDE3B	-0.68318	8.73E-07	5.17E-05	-4.99695	Down	phosphodiesterase 3B
COL7A1	-0.7674	9.21E-07	5.42E-05	-4.98585	Down	collagen type VII alpha 1 chain
HEPACAM2	-0.65213	1.02E-06	5.93E-05	-4.96469	Down	HEPACAM family member 2
CELSR1	-0.64047	1.12E-06	6.39E-05	-4.94638	Down	cadherin EGF LAG seven-pass G-type receptor 1
ZBTB39	-0.67388	1.13E-06	6.46E-05	-4.94372	Down	zinc finger and BTB domain containing 39
MOB3B	-0.68472	1.25E-06	7.03E-05	-4.92272	Down	MOB kinase activator 3B

(Continued)

Table 1. (Continued)

GENE SYMBOL	LOGFC	P VALUE	ADJ.P.VAL	T VALUE	REGULATION	GENE NAME
RHAG	-0.8349	1.26E-06	7.06E-05	-4.92115	Down	Rh associated glycoprotein
CR1	-0.65192	1.32E-06	7.32E-05	-4.91176	Down	complement C3b/C4b receptor 1 (Knops blood group)
DBP	-0.65426	1.38E-06	7.62E-05	-4.90202	Down	D-box binding PAR bZIP transcription factor
TUBGCP6	-0.66735	1.55E-06	8.4E-05	-4.8776	Down	tubulin gamma complex associated protein 6
ZNF549	-0.69296	1.59E-06	8.58E-05	-4.87232	Down	zinc finger protein 549
CSF1R	-0.63553	1.62E-06	8.71E-05	-4.86868	Down	colony stimulating factor 1 receptor
EPB42	-0.87201	1.73E-06	9.24E-05	-4.85526	Down	erythrocyte membrane protein band 4.2
SCARNA7	-0.63099	1.87E-06	9.88E-05	-4.83874	Down	small Cajal body-specific RNA 7
GNG7	-0.66304	1.98E-06	0.000104	-4.82656	Down	G protein subunit gamma 7
ZNF589	-0.63146	2E-06	0.000105	-4.82428	Down	zinc finger protein 589
GCNT2	-0.69581	2.01E-06	0.000105	-4.82357	Down	glucosaminyl (N-acetyl) transferase 2 (I blood group)
GPR146	-0.72697	2.04E-06	0.000106	-4.82048	Down	G protein-coupled receptor 146
QSOX2	-0.66298	2.14E-06	0.000109	-4.8106	Down	quiescin sulfhydryl oxidase 2
SNORA53	-0.92118	2.21E-06	0.000113	-4.80308	Down	small nucleolar RNA, H/ACA box 53
SCARNA13	-0.77859	2.26E-06	0.000115	-4.79894	Down	small Cajal body-specific RNA 13
ITGB2-AS1	-0.62011	3.09E-06	0.000151	-4.73185	Down	ITGB2 antisense RNA 1
ESPN	-0.78256	3.11E-06	0.000152	-4.73085	Down	espin
NEAT1	-0.72879	3.35E-06	0.000162	-4.71479	Down	nuclear paraspeckle assembly transcript 1
FHDC1	-0.93149	3.52E-06	0.000169	-4.70423	Down	FH2 domain containing 1
ZC3H12D	-0.64158	3.53E-06	0.000169	-4.70345	Down	zinc finger CCCH-type containing 12D
ABCD2	-0.6691	3.76E-06	0.000178	-4.6898	Down	ATP binding cassette subfamily D member 2
MCOLN1	-0.69108	3.83E-06	0.000181	-4.68576	Down	mucolipin 1
NR4A1	-0.64016	4.23E-06	0.000196	-4.66458	Down	nuclear receptor subfamily 4 group A member 1
SLC25A42	-0.63249	4.54E-06	0.000209	-4.64904	Down	solute carrier family 25 member 42
GYPA	-0.73764	5.3E-06	0.000239	-4.61504	Down	glycophorin A (MNS blood group)
SCARNA2	-0.67524	6.79E-06	0.000297	-4.5607	Down	small Cajal body-specific RNA 2
FAM167A	-0.65735	7.44E-06	0.000319	-4.54065	Down	family with sequence similarity 167 member A
ALDH6A1	-0.6308	8.11E-06	0.000345	-4.52128	Down	aldehyde dehydrogenase 6 family member A1
CD4	-0.62279	8.14E-06	0.000345	-4.52057	Down	CD4 molecule
ABCA2	-0.6866	9.04E-06	0.000378	-4.49716	Down	ATP binding cassette subfamily A member 2
BEND4	-0.64725	9.32E-06	0.000388	-4.49036	Down	BEN domain containing 4
CENPF	-0.7335	1.03E-05	0.000422	-4.46818	Down	centromere protein F
CD6	-0.65075	1.03E-05	0.000423	-4.46737	Down	CD6 molecule
KLHL3	-0.63143	1.15E-05	0.000465	-4.44229	Down	kelch like family member 3
GYPB	-0.73759	1.45E-05	0.00056	-4.39099	Down	glycophorin B (MNS blood group)
ABCC13	-0.70835	1.46E-05	0.000566	-4.38865	Down	ATP binding cassette subfamily C member 13 (pseudogene)
ATP13A1	-0.61946	1.58E-05	0.000606	-4.3702	Down	ATPase 13A1
MYO15B	-0.6612	1.65E-05	0.000624	-4.36062	Down	myosin XVB
CD5	-0.65427	1.89E-05	0.000697	-4.32962	Down	CD5 molecule
DUSP2	-0.64467	1.91E-05	0.000702	-4.32778	Down	dual specificity phosphatase 2
SCML4	-0.63141	1.91E-05	0.000702	-4.32734	Down	Scmpolycomb group protein like 4
PIK3IP1	-0.62444	3.82E-05	0.001247	-4.16463	Down	phosphoinositide-3-kinase interacting protein 1
ALAS2	-0.66726	5.72E-05	0.001735	-4.06777	Down	5'-aminolevulinate synthase 2
RMRP	-0.64882	8.71E-05	0.002461	-3.96458	Down	RNA component of mitochondrial RNA processing endoribonuclease
RNF182	-0.84789	0.000111	0.00298	-3.90357	Down	ring finger protein 182
RNA5-8SN2	-1.28453	0.000116	0.003077	-3.89329	Down	RNA, 5.8S ribosomal N2
SELENBP1	-0.63971	0.000122	0.003212	-3.87967	Down	selenium binding protein 1
LINC01857	-0.67006	0.000136	0.003506	-3.85285	Down	long intergenic non-protein coding RNA 1857
SCARNA5	-0.67276	0.00026	0.005928	-3.68493	Down	small Cajal body-specific RNA 5
HBM	-0.66252	0.001557	0.024934	-3.18581	Down	hemoglobin subunit mu
TUBB1	-0.63203	0.002292	0.033535	-3.06938	Down	tubulin beta 1 class VI

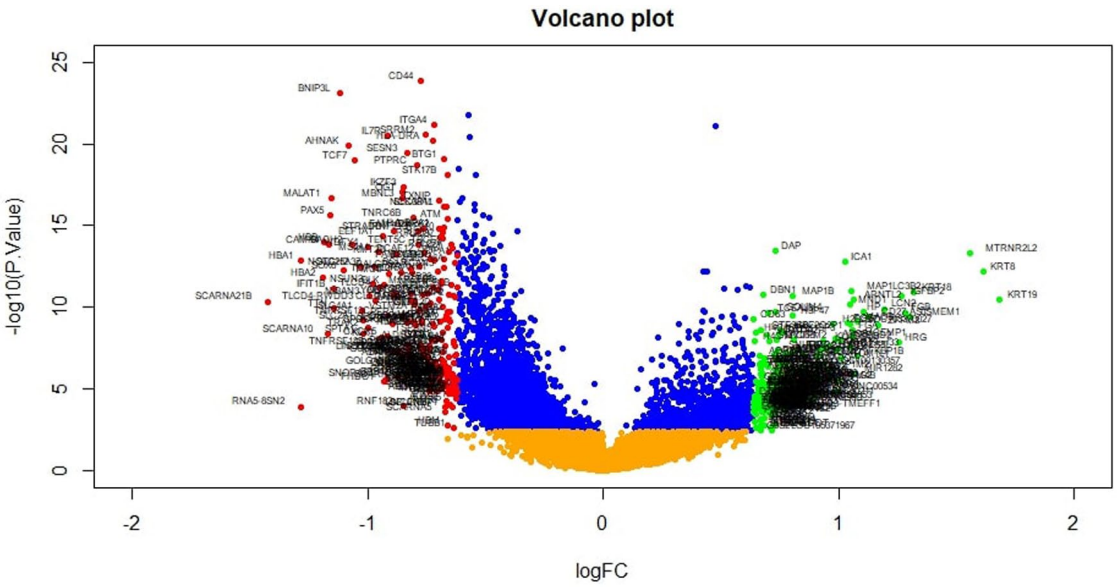

Figure 1. Volcano plot of differentially expressed genes. Genes with a significant change of more than 2-fold were selected. Green dot represented upregulated significant genes and red dot represented downregulated significant genes.

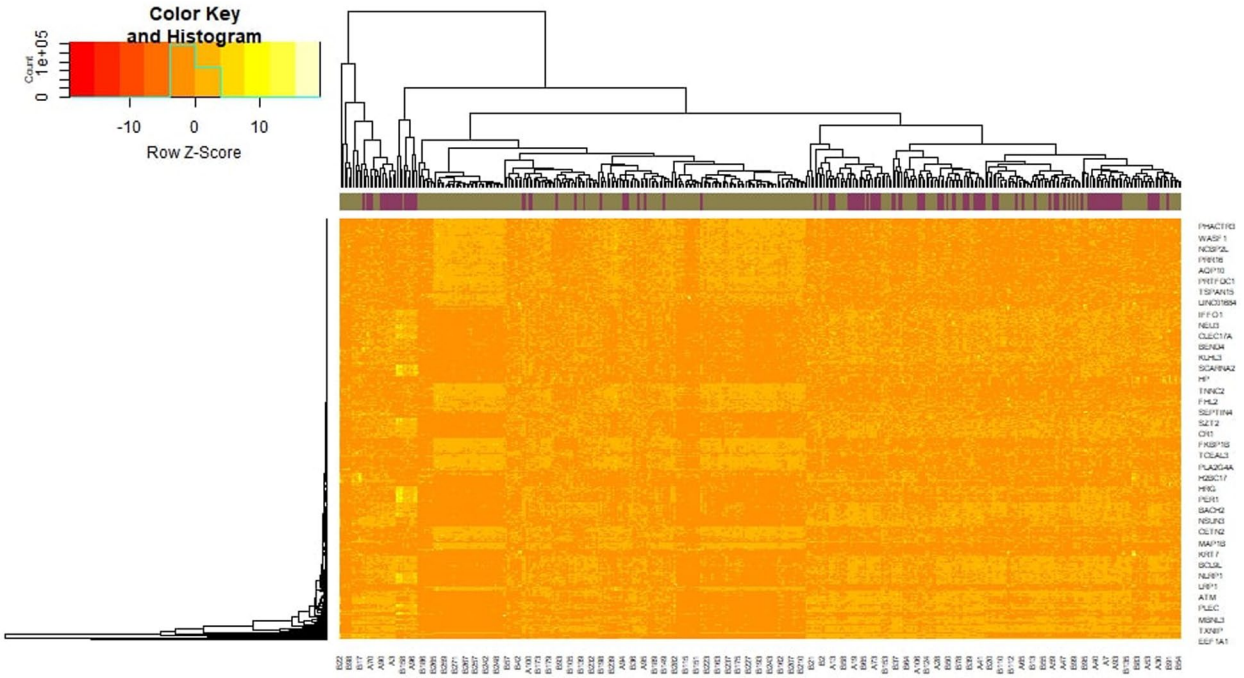

Figure 2. Heat map of differentially expressed genes. Legend on the top left indicates log fold change of genes. (A1-A114 = normal control samples; B1-B284 = PDAC samples). PDAC indicates pancreatic ductal adenocarcinoma.

Construction of miRNA-DEG regulatory network

The regulatory network of miRNA-DEG and predicted targets is presented in Figure 4A. Microtubule-associated protein 1B (*MAP1B*) was modulated by 202 miRNAs (eg, hsa-mir-4461), *CCNB1* that was modulated by 94 miRNAs (eg, hsa-mir-3928-3p), AHNAK nucleoprotein (*AHNAK*) that was modulated by 256 miRNAs (eg, hsa-mir-2682-5p), and lysine methyltransferase 2D (*KMT2D*) that was modulated by 209 miRNAs (ex: hsa-mir-1202) are listed in Table 5. As a group, a total of 257 of the 463 DEGs were contained in the miRNA-DEG regulatory network.

Construction of TF-DEG regulatory network

The regulatory network of TF-DEG and predicted targets is presented in Figure 4B. Enhancer of zeste 2 polycomb repressive complex 2 subunit (*EZH2*) that was modulated by 45 TFs (eg, SRY-box transcription factor 2 [SOX2]), tropomyosin 1 (*TPM1*) that was modulated by 40 TFs (eg, MYC

Table 2. The enriched GO terms of the up and down regulated differentially expressed genes.

GO ID	CATEGORY	GO NAME	P VALUE	FDR B&H	FDR B&Y	BONFERRONI	GENE COUNT	GENE
Up regulated genes								
GO:0016050	BP	vesicle organization	3.92E-07	8.10E-04	7.19E-03	1.58E-03	40	LAPTM4B,CEACAM6,PTGER3,DEFA1,MAGI2,SERPINE2,GLA,PTPRN,HP,VNN1,SPHK1,FGA,FGB,HRG,PLA2G4A,LOXL3,FGG,RAB32,WASF1,VEGFC,UNC13B,PGLYRP1,SEPTIN4,ANXA3,GRK4,APOA2,APOB,LCN2,APOH,DERA,SCARF1,TGFB3,ORM1,TIMP1,MS4A3,CYSTM1,CD63,ERC2,CD151,MCEMP1
GO:0046903	BP	secretion	5.39E-06	1.17E-03	1.04E-02	2.18E-02	38	MYOM1,MAOB,CEACAM6,MDK,PTGER3,DEFA1,SERPINE2,GLA,PTPRN,HP,VNN1,SPHK1,FGA,FGB,HRG,PLA2G4A,FGG,FKBP1B,VEGFC,UNC13B,PGLYRP1,SEPTIN4,ANXA3,ICA1,APOA2,LCN2,APOH,DERA,ARG2,TGFB3,ORM1,OXTR,TIMP1,MS4A3,CYSTM1,CD63,ERC2,MCEMP1
GO:0099503	CC	secretory vesicle	1.01E-08	4.90E-06	3.31E-05	4.90E-06	32	CEACAM6,DEFA1,SERPINE2,GLA,PTPRN,HP,VNN1,SPHK1,FGA,FGB,HRG,PLA2G4A,FGG,VEGFC,UNC13B,PGLYRP1,SEPTIN4,ANXA3,ICA1,RABAC1,LCN2,APOH,DERA,TGFB3,MAL2,ORM1,TIMP1,MS4A3,CYSTM1,CD63,SMPD1,MCEMP1
GO:0098805	CC	whole membrane	2.77E-03	3.64E-02	2.47E-01	1.00E+00	29	TSPAN15,MAOB,LAPTM4B,CEACAM6,FUNDC1,PTPRN,MAP1LC3B2,VNN1,SPHK1,GOLIM4,HRG,RAB32,WASF1,UNC13B,SEPTIN4,ANXA3,ICA1,TOM1L1,AP1M2,GRB14,APOB,RET,SCARF1,MAL2,MS4A3,CYSTM1,CD63,CTNS,MCEMP1
GO:0046983	MF	protein dimerization activity	4.40E-04	9.54E-02	6.73E-01	2.86E-01	30	TPM1,TPM2,PADI4,MYOM1,MAOB,TRPC6,ACOT7,CEACAM6,ARNTL2,PRTFDC1,TYMS,H2AC13,H2BC17,GLA,HP,H4C14,MITF,PKD2,FGG,H2BC11,TPST1,SEPTIN4,ICA1,H4C15,GRB14,E2F1,APOA2,LCN2,TGFB3,H2AJ
GO:0005102	MF	signaling receptor binding	4.71E-03	2.10E-01	1.00E+00	1.00E+00	30	MDK,MTRNR2L2,MAGI2,SERPINE2,GLA,PKD2,FGA,FGB,HRG,FGG,FHL2,FKBP1B,VEGFC,PROK2,PGLYRP1,CMTM2,GRB14,LAMB2,APOA2,APOB,ADAMTS5,CXCL3,ADAM22,CCNB1,TGFB1I1,TGFB3,BCAP31,IGFBP2,TIMP1,CD151
Down regulated genes								
GO:0046649	BP	lymphocyte activation	1.37E-15	5.40E-12	4.78E-11	5.40E-12	40	HLA-DMB,HLA-DPA1,SPTA1,BCL11A,ITGA4,FGL2,CXCR5,FCRL1,PTPRC,ZC3H12D,FBXO7,CCR7,NOTCH2,TCF7,IKZF3,POLM,CAMK4,POU2F2,BTLA,CR1,CBLB,SLC4A1,TFRC,BCL11B,CD4,CD5,CD6,MS4A1,CD22,CD27,CD44,TNFRSF13C,TNFRSF13B,CD79A,RORA,ATM,LY9,LEF1,IL7R,NCKAP1L

(Continued)

Table 2. (Continued)

GO ID	CATEGORY	GO NAME	P VALUE	FDR B&H	FDR B&Y	BONFERRONI	GENE COUNT	GENE
GO:0010941	BP	regulation of cell death	9.53E-05	6.03E-03	5.34E-02	3.75E-01	40	STK17B,OBSCN,ITGA4,NR4A1,STRADB,BNIP3L,PTPRC,BTG1,TMC8,FBXO7,PLAGL2,CCR7,NOTCH2,TCF7,IKZF3,OGT,CAMK1D,BMF,NLRP1,GRINA,OPA1,EEF1A1,TXNIP,BCL11B,IGF2R,CSF1R,CD27,NEURL1,CD44,LRP1,ATM,HBA1,HBA2,HBB,CTSB,LEF1,RPL10,IL7R,SORL1,NCKAP1L
GO:0009986	CC	cell surface	2.02E-09	3.10E-07	2.08E-06	9.30E-07	35	ADAM19,HLA-DPA1,HLA-DRA,ITGA4,CXCR5,FCRL1,PTPRC,CIITA,MRC2,CCR7,NOTCH2,SEMA7A,BTLA,CR1,SLC4A1,TFRC,CD4,CD5,IGF2R,CD6,CSF1R,MS4A1,CLEC17A,CD22,CD27,GYPA,VCAN,CD44,CLEC2D,TNFRSF13C,TNFRSF13B,CD79A,LY9,CTSB,IL7R
GO:0031226	CC	intrinsic component of plasma membrane	5.35E-07	4.11E-05	2.76E-04	2.47E-04	43	HLA-DPA1,HLA-DRA,SPTA1,SLC38A5,ITGA4,SLC38A1,CXCR5,PTPRC,SLC24A4,TMC8,NOTCH2,VIPR1,TRABD2A,SEMA7A,BTLA,SLC7A6,CR1,MCOLN1,SLC2A1,TSPAN5,RHAG,SLC4A1,TFRC,CELSR1,CD4,CD5,IGF2R,CD6,CSF1R,P2RX5,MS4A1,SLC14A1,CD22,CD27,GYPA,GYPB,CD44,CLEC2D,LRP1,TNFRSF13B,ATP2B1,SORL1,NCKAP1L
GO:0016772	MF	transferase activity, transferring phosphorus-containing groups	9.72E-04	4.32E-02	3.09E-01	6.92E-01	35	ZBTB20,RPS6KA5,STK17B,OBSCN,TENT5C,TTN,PIK3IP1,BLK,STRADB,PTPRC,CIITA,FBXO7,CCR7,DYRK2,OGT,CAMK1D,CTC1,POLM,CAMK4,DUSP2,AAK1,CBLB,SLC4A1,EEF1A1,RMRP,CD4,IGF2R,CSF1R,NEURL1,CD44,LRP1,ATM,SERINC5,SORL1,NCKAP1L
GO:0008144	MF	drug binding	1.15E-02	1.55E-01	1.00E+00	1.00E+00	30	ABCA2,RPS6KA5,STK17B,OBSCN,TTN,BLK,STRADB,CIITA,ALAS2,ABCD2,DYRK2,DNHD1,ACSL6,CAMK1D,EP400,ATP13A1,CAMK4,AAK1,NLRP1,EEF1A1,DNAH1,CSF1R,P2RX5,ATM,HBA1,HBA2,HBM,HBB,ATP2B1,EPB42

Biological Process(BP), Cellular Component(CC) and Molecular Functions (MF).

Table 3. The enriched pathway terms of the up and down regulated differentially expressed genes.

PATHWAY ID	PATHWAY NAME	P-VALUE	FDR B&H	FDR B&Y	BONFERRONI	GENE COUNT	GENE
Up regulated genes							
1269340	Hemostasis	4.28E-06	7.47E-04	5.11E-03	2.24E-03	22	GNG8,TRPC6,CEACAM6,CABLES1,SERPINE2,FGA,KCNMB1,FGB,HRG,PLA2G4A,MMP1,FGG,VEGFC,GRB14,APOB,APOH,ZFPM2,TGFB3,ORM1,TIMP1,CD63,PRKAR1B
1269741	Cell Cycle	8.91E-04	2.12E-02	1.45E-01	4.67E-01	17	CETN2,MND1,MCM10,GINS1,TYMS,H2BC17,H4C14,BUB1,H2BC11,UBE2C,H4C15,CENPU,E2F1,CCNB1,DMC1,CENPI,H2AJ
1269507	Signaling by Rho GTPases	1.14E-02	8.42E-02	5.76E-01	1.00E+00	11	PPP1R14A,TAX1BP3,H2BC17,H4C14,BUB1,WASF1,H2BC11,H4C15,CENPU,CENPI,H2AJ
1269203	Innate Immune System	7.89E-02	2.91E-01	1.00E+00	1.00E+00	21	CEACAM6,DEFA1,GLA,HP,VNN1,FGA,FGB,FGG,WASF1,PGLYRP1,APOB,RET,LCN2,POLR3G,DERA,ORM1,MS4A3,CYSTM1,CD63,PRKAR1B,MCEMP1
1270001	Metabolism of lipids and lipoproteins	1.52E-01	3.82E-01	1.00E+00	1.00E+00	13	ACER2,ACOT7,ME1,GLA,SPHK1,PLA2G4A,FHL2,PLAAT1,G0S2,THEM5,APOA2,APOB,SMPD1
1268677	Metabolism of proteins	3.37E-01	5.01E-01	1.00E+00	1.00E+00	21	GNG8,CETN2,FN3K,H2AC13,H2BC17,VNN1,SPHK1,H4C14,MITF,FGA,MMP1,RAB32,METTL22,DYNC1I1,H2BC11,ADAMTS1,UBE2C,H4C15,ADAMTS5,IGFBP2,AOPEP
Down regulated genes							
1269171	Adaptive Immune System	1.59E-03	8.64E-02	5.87E-01	7.96E-01	20	HLA-DMB,HLA-DPA1,HLA-DRA,TNRC6B,ITGA4,NR4A1,BLK,KLHL3,PTPRC,MRC2,FBXO7,RNF213,BTLA,CBLB,CD4,CD22,CLEC2D,CD79A,CTSB,RNF182
1269903	Transmembrane transport of small molecules	1.39E-02	1.95E-01	1.00E+00	1.00E+00	15	ABCA2,SLC38A5,SLC38A1,SLC24A4,ABCD2,GNG7,ATP13A1,SLC7A6,MCOLN1,SLC2A1,RHAG,SLC4A1,TFRC,SLC14A1,ATP2B1
1269203	Innate Immune System	8.82E-02	4.76E-01	1.00E+00	1.00E+00	21	RPS6KA5,SPTA1,TNRC6B,NR4A1,ADA2,FGL2,PTPRC,CAMK4,DUSP2,NLRP1,CNKSR2,CR1,EEF1A1,TXNIP,EEF2,CD4,IGF2R,CD44,HBB,CTSB,NCKAP1L
1269876	Vesicle-mediated transport	1.54E-01	5.50E-01	1.00E+00	1.00E+00	11	SPTA1,SEC16A,COL7A1,AAK1,TFRC,CD4,IGF2R,LRP1,HBA1,HBA2,HBB
1268854	Disease	3.21E-01	6.43E-01	1.00E+00	1.00E+00	12	RPL23A,RPL27A,RPL37,NR4A1,NOTCH2,CNKSR2,EEF2,CD4,VCAN,NEURL1,RPL13A,RPL10
1268677	Metabolism of proteins	5.53E-01	7.60E-01	1.00E+00	1.00E+00	19	RPL23A,RPL27A,RPL37,SPTA1,MGAT4A,NEU3,ADA2,TUBB1,YOD1,SEC16A,GNG7,KLK1,COL7A1,OGT,EEF1A1,EEF2,RPL13A,RPL10,SORL1

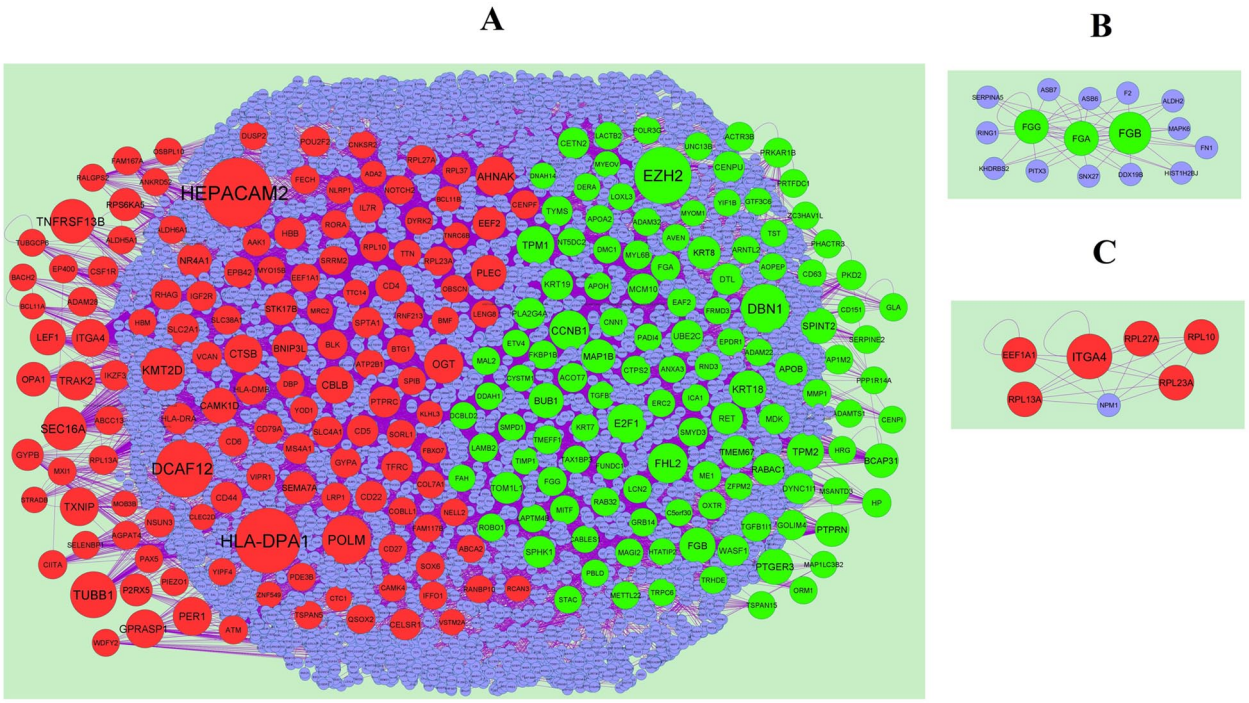

Figure 3. PPI network and the most significant modules of DEGs. (A) The PPI network of DEGs was constructed using Cytoscape; (B) the most significant module was obtained from PPI network with 16 nodes and 44 edges for upregulated genes; (C) the most significant module was obtained from PPI network with 6 nodes and 20 edges for upregulated genes. Upregulated genes are marked in green; downregulated genes are marked in red. DEGs indicate differentially expressed genes; PPI, protein-protein interaction network.

proto-oncogene, bHLH transcription factor [MYC]), *AHNAK* that was modulated by 58 TFs (eg, KLF4), and thioredoxin interacting protein (TXNIP) that was modulated by 51 TFs (eg, tumor protein p63 [TP63]) are listed in Table 5. As a group, a total of 259 of the 463 DEGs were contained in the TF-DEG regulatory network.

Validation of hub genes

All of the hub genes were validated in TCGA data. Hub genes contributed to the survival period in patients with PDAC, and we analyzed the overall survival (OS) for each hub gene by UALCAN (Figure 5). The results showed that the high expression of *CCNB1* and *FHL2* mRNA level was associated with the worse OS in patients with PDAC, while low expression of *HLA-DPA1* and *TUBB1* mRNA level was associated with the worse OS in patients with PDAC. As shown in Figure 6, the expression of the upregulated hub genes *CCNB1* and *FHL2* in PDAC was significantly elevated compared with normal, while expression of the downregulated hub genes *HLA-DPA1* and *TUBB1* in PDAC was significantly decreased compared with normal. The expression of each hub gene in PDAC patients was analyzed according to the individual cancer stage. As shown in Figure 7, the expression of *CCNB1* and *FHL2* were higher in patients with all individual cancer stages than that in normal, which revealed that these upregulated hub genes might be associated with tumor progression positively, whereas the expression of *HLA-DPA1* and *TUBB1* were lower in patients with all individual cancer stages than that in normal, which revealed that these downregulated hub genes might be associated with tumor progression positively. We used cBioportal tool to explore the specific mutation of hub genes in PDAC data set with 184 samples. From the OncoPrint, percentages of alterations in *CCNB1, FHL2, HLA-DPA1*, and *TUBB1* genes among lung cancer ranged from 0% to 2.3% in individual genes (*CCNB1*, 0%; *FHL2*, 0.6%; *HLA-DPA1*, 2.3%; *TUBB1*, 2.3%) and are shown in Figure 8. In addition, we used the "HPA" to examine the protein expression levels of *CCNB1* and *FHL2*, and found that the protein expression levels of the these hub genes were noticeably upregulated in PDAC compared with normal tissues, whereas protein expression levels of *HLA-DPA1* and *TUBB1* were noticeably downregulated in PDAC compared with normal tissues (Figure 9). The association of *CCNB1, FHL2, HLA-DPA1*, and *TUBB1* expression level with immune infiltration abundance in PDAC was evaluated using TIMER database. *CCNB1* and *FHL2* expression were negatively correlated with infiltration degree of B cells, CD8+ T cells, macrophage, neutrophil, and dendritic cells, whereas *HLA-DPA1* and *TUBB1* were positively correlated with infiltration degree of B cells, CD8+ T cells, macrophage, neutrophil, and dendritic cells and are shown in Figure 10. As these 4 genes are prominently expressed in PDAC, we performed an ROC curve analysis to evaluate their sensitivity and specificity for the diagnosis of PDAC. As shown in Figure 11, *CCNB1, FHL2, HLA-DPA1*, and *TUBB1* achieved an AUC value of >0.70, demonstrating that these genes have high sensitivity

Table 4. Topology table for up and down regulated genes.

REGULATION	NODE	DEGREE	BETWEENNESS	STRESS	CLOSENESS
Up	*EZH2*	350	0.076224	81130962	0.349924
Up	*DBN1*	256	0.049032	39941040	0.348151
Up	*CCNB1*	158	0.024471	43653864	0.313488
Up	*FHL2*	158	0.031673	16397718	0.336762
Up	*E2F1*	151	0.025971	16601668	0.333208
Up	*TPM1*	134	0.022043	16976362	0.329604
Up	*KRT18*	132	0.018793	17362522	0.338383
Up	*TPM2*	126	0.021531	17717608	0.323503
Up	*FGB*	115	0.021143	15804232	0.298889
Up	*PTGER3*	113	0.019531	25585198	0.284342
Up	*SPINT2*	108	0.023415	14310762	0.303448
Up	*BUB1*	102	0.018982	9083534	0.319527
Up	*PTPRN*	93	0.015139	21217898	0.283912
Up	*BCAP31*	91	0.017733	11925460	0.323825
Up	*MAP1B*	91	0.011535	22589676	0.310858
Up	*KRT8*	79	0.009251	9231600	0.332081
Up	*TMEM67*	76	0.014065	4982016	0.290838
Up	*RABAC1*	74	0.013172	9708740	0.293098
Up	*APOB*	72	0.011818	15182272	0.302587
Up	*UBE2C*	69	0.00877	8892764	0.298716
Up	*SPHK1*	68	0.011494	4951244	0.325666
Up	*TOM1L1*	66	0.00895	6727694	0.305124
Up	*RET*	66	0.009723	10964184	0.305199
Up	*WASF1*	65	0.010329	14175172	0.29873
Up	*KRT19*	64	0.008418	5490710	0.32224
Up	*CENPU*	61	0.011081	3633098	0.296468
Up	*DTL*	61	0.006526	9721978	0.297152
Up	*CETN2*	60	0.009249	16418248	0.269586
Up	*MCM10*	59	0.007694	9107150	0.300602
Up	*DYNC1I1*	58	0.007347	6841812	0.299279
Up	*PLA2G4A*	57	0.006497	7102868	0.307673
Up	*TYMS*	55	0.008254	2898568	0.306378
Up	*MDK*	54	0.007633	2641060	0.307322
Up	*GOLIM4*	45	0.009056	6535396	0.299091
Up	*TGFB1I1*	43	0.00576	2542056	0.317363
Up	*PKD2*	42	0.006903	2134988	0.290538

(Continued)

Table 4. (Continued)

REGULATION	NODE	DEGREE	BETWEENNESS	STRESS	CLOSENESS
Up	*FGA*	41	0.004439	1801264	0.293153
Up	*PRKAR1B*	41	0.004763	4851900	0.299424
Up	*ACOT7*	39	0.00511	6777086	0.287968
Up	*FGG*	37	0.002736	1188570	0.282125
Up	*AP1M2*	37	0.007088	9431672	0.281894
Up	*MITF*	36	0.006067	5049390	0.308118
Up	*SMYD3*	35	0.006122	1971838	0.303776
Up	*ACTR3B*	35	0.002767	5762182	0.273907
Up	*CTPS2*	34	0.004516	1656234	0.297352
Up	*HP*	33	0.004002	2476788	0.299743
Up	*MYL6B*	33	0.001721	1494552	0.303835
Up	*LAMB2*	33	0.003266	3787290	0.283015
Up	*ME1*	32	0.00497	5458746	0.266142
Up	*FKBP1B*	31	0.002492	3149134	0.263535
Up	*EAF2*	31	0.003666	3614748	0.273181
Up	*CD63*	30	0.002963	1542292	0.278807
Up	*TMEFF1*	29	0.004306	1459454	0.277382
Up	*PHACTR3*	29	0.003235	6793662	0.273205
Up	*MMP1*	28	0.004131	1062610	0.285972
Up	*RAB32*	28	0.004125	3089688	0.273326
Up	*NT5DC2*	27	0.003149	4016356	0.290497
Up	*LAPTM4B*	26	0.003861	1308630	0.280985
Up	*LCN2*	26	0.003047	3293226	0.261121
Up	*GRB14*	26	0.001737	2102726	0.272171
Up	*PRTFDC1*	26	0.003559	2778424	0.248364
Up	*SERPINE2*	25	0.003606	2767974	0.266199
Up	*APOA2*	24	0.003639	1777538	0.282035
Up	*CNN1*	24	0.002696	1398988	0.281984
Up	*MAGI2*	24	0.003636	4072986	0.273277
Up	*PADI4*	24	0.001853	2786250	0.285457
Up	*ARNTL2*	23	0.004537	2736046	0.276156
Up	*MAL2*	23	0.004035	3057928	0.266555
Up	*TAX1BP3*	22	0.00296	2483404	0.27773
Up	*APOH*	22	0.002261	1011952	0.294759
Up	*GLA*	22	0.002185	2812520	0.25131
Up	*KRT7*	22	0.002247	3354252	0.283132

(Continued)

Table 4. (Continued)

REGULATION	NODE	DEGREE	BETWEENNESS	STRESS	CLOSENESS
Up	*ROBO1*	22	0.002997	2829202	0.285181
Up	*ADAMTS1*	21	0.003523	2991386	0.249044
Up	*OXTR*	21	0.003005	1885024	0.254274
Up	*ADAM32*	21	0.002751	2226220	0.244362
Up	*TSPAN15*	20	0.002903	1636154	0.248684
Up	*DMC1*	20	0.001518	1667540	0.255218
Up	*EPDR1*	20	0.00263	955076	0.289735
Up	*LACTB2*	20	0.003285	3861294	0.241888
Up	*UNC13B*	19	0.003409	6715552	0.228252
Up	*ERC2*	19	0.002956	2368572	0.246592
Up	*HRG*	19	0.002437	1023636	0.273991
Up	*SMPD1*	19	0.00236	2063048	0.275125
Up	*ZFPM2*	19	0.001198	1822000	0.266153
Up	*METTL22*	19	0.001598	2257038	0.269023
Up	*ORM1*	18	0.001349	1072266	0.255461
Up	*ZC3HAV1 L*	18	0.001054	1624786	0.281202
Up	*STAC*	18	0.001798	2388538	0.275578
Up	*POLR3G*	17	0.003237	9664174	0.229055
Up	*DDAH1*	17	0.003704	1699018	0.290824
Up	*TIMP1*	17	0.002047	1211820	0.264888
Up	*DERA*	17	0.001512	1709944	0.240983
Up	*TGFB3*	16	0.001732	1135010	0.26056
Up	*ANXA3*	16	0.002306	3218636	0.263928
Up	*ETV4*	16	0.00158	1430402	0.286767
Up	*RND3*	16	0.001618	1798784	0.267963
Up	*FUNDC1*	16	0.001881	5031262	0.246033
Up	*PPP1R14A*	16	0.001348	1468196	0.269398
Up	*ADAM22*	16	9.66E-04	1467492	0.278092
Up	*TRHDE*	16	0.002417	2718244	0.265571
Up	*AOPEP*	15	5.09E-04	455628	0.281778
Up	*LOXL3*	15	0.002245	2647672	0.272735
Up	*TST*	15	0.002644	2760934	0.24058
Up	*CENPI*	15	6.90E-04	213372	0.26143
Up	*TRPC6*	15	0.002982	3195972	0.236597
Up	*MSANTD3*	14	0.001423	599870	0.282602
Up	*DCBLD2*	14	0.001863	1414006	0.280806

(Continued)

Table 4. (Continued)

REGULATION	NODE	DEGREE	BETWEENNESS	STRESS	CLOSENESS
Up	*ICA1*	14	0.001837	1818980	0.253566
Up	*CABLES1*	14	4.42E-04	448806	0.275222
Up	*GTF3C6*	13	0.001446	393772	0.300413
Up	*AVEN*	13	7.46E-04	364352	0.294788
Up	*PBLD*	13	0.001491	1062854	0.235839
Up	*CD151*	13	0.001883	1879220	0.264662
Up	*YIF1B*	13	0.001267	1419634	0.263917
Up	*C5orf30*	13	0.001783	1452154	0.265582
Up	*FRMD3*	11	8.55E-04	686546	0.235579
Up	*FAH*	11	0.001509	1294972	0.259587
Up	*HTATIP2*	11	0.00148	1272602	0.261231
Up	*CYSTM1*	11	0.002293	1438306	0.2152
Up	*MAP1LC3B2*	10	0.001139	1052378	0.240608
Up	*MYEOV*	2	5.45E-05	24642	0.227079
Up	*DNAH14*	1	0	0	0.212349
Up	*MYOM1*	1	0	0	0.247539
Down	*HEPACAM2*	496	0.004088	4614336	0.259565
Down	*HLA-DPA1*	443	0.021345	6656236	0.294395
Down	*DCAF12*	359	0.002195	1838728	0.28738
Down	*POLM*	259	6.45E-05	60748	0.246809
Down	*TUBB1*	231	0.017014	13445244	0.31686
Down	*KMT2D*	211	0.004121	6143304	0.276119
Down	*TNFRSF13B*	208	0.004558	7473486	0.25441
Down	*SEC16A*	199	0.024345	23456762	0.332778
Down	*AHNAK*	158	0.012868	12992410	0.339572
Down	*OGT*	151	0.02538	23785672	0.321486
Down	*TRAK2*	148	0.005447	1889278	0.291359
Down	*PER1*	143	0.007889	3343992	0.297667
Down	*TXNIP*	142	0.005831	3723272	0.3011
Down	*GPRASP1*	140	0.011046	5269570	0.284316
Down	*CTSB*	139	0.011516	5746824	0.316973
Down	*ITGA4*	132	0.110358	99169576	0.373747
Down	*CBLB*	131	0.011859	9651222	0.31117
Down	*LEF1*	111	0.008924	3863000	0.305275
Down	*PLEC*	110	0.025923	21209448	0.346999
Down	*BNIP3L*	110	0.005843	2394548	0.292184

(Continued)

Table 4. (Continued)

REGULATION	NODE	DEGREE	BETWEENNESS	STRESS	CLOSENESS
Down	*CAMK1D*	109	0.007993	5854240	0.294255
Down	*NR4A1*	99	0.024611	10885038	0.333639
Down	*OPA1*	94	0.007387	5152054	0.317804
Down	*EEF2*	83	0.037887	47075150	0.354698
Down	*SEMA7A*	82	0.00308	4153990	0.271146
Down	*RPS6KA5*	78	0.010004	5767566	0.321653
Down	*STK17B*	78	0.00446	1356036	0.284918
Down	*P2RX5*	75	0.003754	3579124	0.255008
Down	*SLC2A1*	68	0.003791	2359116	0.318622
Down	*GYPB*	66	0.007619	6671358	0.262863
Down	*HBB*	65	0.01032	10858208	0.304059
Down	*CD22*	64	0.001809	1124092	0.279752
Down	*CD4*	64	0.018753	14195846	0.322845
Down	*CD44*	63	0.031474	16859342	0.344469
Down	*TFRC*	63	0.019104	17774714	0.337221
Down	*PTPRC*	62	0.012352	6796924	0.316681
Down	*CD5*	62	0.00189	1129318	0.283456
Down	*HLA-DRA*	61	0.009348	4428892	0.287995
Down	*HLA-DMB*	60	0.002503	1238774	0.277344
Down	*CELSR1*	60	0.003079	1745004	0.272928
Down	*MS4A1*	58	0.0017	1236694	0.276378
Down	*SPTA1*	55	0.007158	4511084	0.30275
Down	*IL7R*	54	0.027811	45141856	0.327043
Down	*GYPA*	53	8.14E-04	390278	0.260045
Down	*SLC4A1*	53	0.002142	1341058	0.273169
Down	*EPB42*	52	0.002323	1787000	0.260879
Down	*RHAG*	49	0	0	0.214566
Down	*CD79A*	49	0.008789	4491848	0.293056
Down	*CD6*	48	0	0	0.220862
Down	*CSF1R*	48	0.002723	5503564	0.281868
Down	*IKZF3*	48	0.021447	15624140	0.316487
Down	*POU2F2*	46	0.002814	4242740	0.262773
Down	*IGF2R*	45	0.005336	8354606	0.300049
Down	*NSUN3*	45	0	0	0.226647
Down	*BLK*	44	0.009001	4827382	0.309644
Down	*VCAN*	44	0.00605	2854094	0.288546

(Continued)

Table 4. (Continued)

REGULATION	NODE	DEGREE	BETWEENNESS	STRESS	CLOSENESS
Down	*ADAM28*	41	0	0	0.272076
Down	*RPL27A*	41	0.009338	13186584	0.337921
Down	*RPL23A*	39	0.022449	25286012	0.35326
Down	*EEF1A1*	37	0.098882	1.23E + 08	0.370457
Down	*RPL13A*	37	0.009659	13645424	0.339386
Down	*RPL10*	35	0.066934	69760500	0.352275
Down	*NOTCH2*	35	0.009449	4095454	0.307291
Down	*ATP2B1*	35	0.00508	5650696	0.303835
Down	*SLC38A1*	35	0.008346	5880382	0.292709
Down	*QSOX2*	35	0.00527	3561792	0.291167
Down	*SORL1*	34	0.01017	6644994	0.299569
Down	*LRP1*	34	0.030447	29146796	0.321269
Down	*SRRM2*	34	0.044661	52105132	0.347662
Down	*ABCC13*	34	0	0	0.250182
Down	*ATM*	33	0.040568	31808618	0.330997
Down	*FECH*	33	0.007383	3340210	0.299511
Down	*CD27*	32	0.004882	2960412	0.278142
Down	*VIPR1*	32	0.004948	5472644	0.278694
Down	*AGPAT4*	32	1.70E-05	28760	0.230987
Down	*CIITA*	32	0.003427	3117716	0.289328
Down	*EP400*	31	0.007237	9601258	0.288196
Down	*RORA*	31	0.004548	1396286	0.302558
Down	*SOX6*	31	0.001788	1768940	0.255661
Down	*CENPF*	30	0.008068	6644598	0.297681
Down	*FAM167A*	29	0.008587	3540932	0.276168
Down	*MXI1*	28	0.001985	3293278	0.269504
Down	*ALDH5A1*	27	0.003494	4468018	0.270813
Down	*RPL37*	27	0.001913	3460916	0.29617
Down	*TSPAN5*	26	0.01221	9998796	0.2873
Down	*PIEZO1*	26	0	0	0.223188
Down	*BTG1*	25	0.002334	3106952	0.271777
Down	*SPIB*	25	0.001073	679476	0.280679
Down	*ALDH6A1*	25	0.00345	3839804	0.246053
Down	*COL7A1*	25	0.003621	3830672	0.277705
Down	*PAX5*	25	0.008408	15230588	0.288317
Down	*DUSP2*	24	0.003694	4774362	0.262573

(Continued)

Table 4. (Continued)

REGULATION	NODE	DEGREE	BETWEENNESS	STRESS	CLOSENESS
Down	*IFFO1*	24	0.004108	2648480	0.262006
Down	*COBLL1*	24	0.00318	3800612	0.267373
Down	*DBP*	24	0.00207	2593884	0.258708
Down	*SELENBP1*	24	0.011965	15173332	0.275259
Down	*DYRK2*	23	0.00992	5736550	0.313918
Down	*PDE3B*	23	0.005858	5188848	0.268242
Down	*ABCA2*	22	0.002246	1887488	0.270647
Down	*TTN*	22	0.022803	22179002	0.328956
Down	*AAK1*	22	0.001768	1776702	0.306636
Down	*CAMK4*	21	0.001804	1122842	0.282382
Down	*ANKRD52*	21	0.004706	3610412	0.290251
Down	*OBSCN*	21	0.002307	1424536	0.295125
Down	*YOD1*	21	0.003727	4452540	0.278581
Down	*RNF213*	21	0.003281	4225796	0.28073
Down	*HBM*	21	0.003971	2893622	0.211891
Down	*FAM117B*	20	0.002939	3060242	0.274465
Down	*RANBP10*	20	0.010162	16110914	0.263344
Down	*RALGPS2*	20	0.008034	10752578	0.280386
Down	*CNKSR2*	19	0.003716	4283878	0.253753
Down	*MYO15B*	19	0.001548	1850770	0.253763
Down	*BMF*	18	0.002348	3575424	0.266842
Down	*WDFY2*	18	0.004928	3808614	0.241237
Down	*LENG8*	18	0.006353	9944066	0.270896
Down	*TUBGCP6*	18	0.00405	3821222	0.278155
Down	*NELL2*	17	0.005907	5985122	0.250435
Down	*YIPF4*	17	0.002754	3249620	0.263928
Down	*OSBPL10*	17	0.002471	663904	0.287727
Down	*BACH2*	16	0.002632	2910574	0.257534
Down	*NLRP1*	16	0.003929	3755972	0.280691
Down	*BCL11B*	2	0.001184	2467486	0.258362
Down	*STRADB*	2	0.001267	1783952	0.276898
Down	*BCL11A*	1	0.004017	6158386	0.273664
Down	*RCAN3*	1	0	0	0.233006
Down	*KLHL3*	1	0.003155	2811806	0.280551
Down	*CLEC2D*	1	0.015351	13153684	0.270766
Down	*TNRC6B*	1	0.010638	19725384	0.302365

(Continued)

Table 4. (Continued)

REGULATION	NODE	DEGREE	BETWEENNESS	STRESS	CLOSENESS
Down	*FBXO7*	1	0.011435	14645282	0.298528
Down	*MOB3B*	1	0	0	0.202401
Down	*ZNF549*	1	0	0	0.230523
Down	*VSTM2A*	1	0	0	0.220343
Down	*CTC1*	1	0	0	0.200285
Down	*MRC2*	1	0.002911	3908206	0.26787
Down	*TTC14*	1	0	0	0.257985
Down	*ADA2*	1	0	0	0.257985

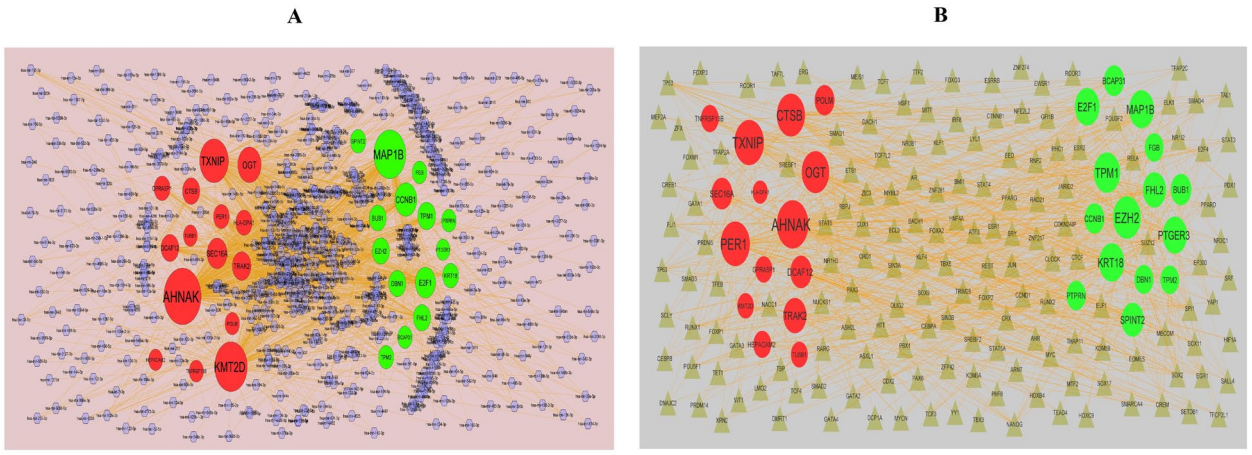

Figure 4. (A) Target gene—miRNA regulatory network between target genes and miRNAs (B) Target gene—TF regulatory network between target genes and TFs. Upregulated genes are marked in green; downregulated genes are marked in red; the blue color diamond nodes represent the key miRNAs; the gray color triangle nodes represent the key TFs.

and specificity for PDAC diagnosis. The results suggested that *CCNB1, FHL2, HLA-DPA1*, and *TUBB1* can be used as biomarkers for the diagnosis of PDAC.

Discussion

Due to the high heterogeneity of PDAC, it was still a disease with high rates of pervasiveness and fatality. With surgery as the main treatment, the other treatments including radiotherapy, chemotherapy, targeted therapy, and gene therapy as a additive to the finite treatment measures of PDAC, the 5-year survival rate was still less than 8%.[35] Therefore, the early diagnosis and effective treatment of PDAC are crucially required, which might be achieved via the identification of the DEGs between PDAC and normal control, and by considering the underlying molecular mechanism. NGS data analysis can screen a massive number of genes in the human genome for further functional analysis, and can be extensively used to screen biomarkers for early diagnosis and unique therapeutic targets. Therefore, they might help the diagnosis and prognosis of PDAC in the early stages and help in advancement of targeted treatment.

The current investigation systematically applied integrated bioinformatics methods to identify novel biomarkers that serve roles in the advancement of PDAC. The data extracted from the GEO data set contained 284 PDAC and 117 normal control samples. A total of 232 upregulated and 231 downregulated genes in PDAC, when compared with normal control samples, were identified using bioinformatics analysis, indicating the incidence and advancement of PDAC. The results of the DEGs might provide potential biomarkers for the diagnosis of PDAC. *DAP* (death associated protein),[36] keratin 8 (*KRT8*),[37] insulin-like growth factor binding protein 2 (*IGFBP2*),[38] keratin 19 (*KRT19*),[39] CD44 molecule (Indian blood group) (*CD44*),[40] *AHNAK*,[41] and BTG anti-proliferation factor 1 (*BTG1*)[42] were the potential gene targets of the drugs for treating PDAC. KIF2C[43] induces proliferation, migration, and invasion in gastric cancer patients through the MAPK signaling pathway. Drebrin 1 (*DBN1*)[44] has been

Table 5. miRNA—target gene and TF—target gene interaction.

REGULATION	TARGET GENES	DEGREE	MICRORNA	REGULATION	TARGET GENES	DEGREE	TF
Up	*COL1A1*	178	hsa-mir-4492	Up	*IRF4*	10	NFATC2
Up	*IRF4*	140	hsa-mir-4319	Up	*LCK*	10	YY1
Up	*MYBL2*	83	hsa-mir-637	Up	*RET*	10	NR2C2
Up	*PRKCB*	81	hsa-mir-1261	Up	*MAP1LC3C*	10	MAX
Up	*IL2RB*	54	hsa-mir-4300	Up	*IL2RB*	8	PDX1
Up	*CCR5*	50	hsa-mir-5193	Up	*GRAP2*	8	ELK1
Up	*GRAP2*	41	hsa-mir-3681-5p	Up	*MYBPC2*	7	RELA
Up	*MDFI*	41	hsa-mir-4441	Up	*MDFI*	6	TFAP2A
Up	*RET*	17	hsa-mir-129-2-3p	Up	*MYBL2*	6	GATA2
Up	*IKZF1*	16	hsa-mir-3607-3p	Up	*CD247*	5	SREBF1
Up	*BTK*	13	hsa-mir-4667-3p	Up	*COL1A1*	5	NFYA
Up	*LCK*	6	hsa-mir-210-3p	Up	*PRKCB*	4	IRF2
Up	*MYBPC2*	6	hsa-mir-214-3p	Up	*IKZF1*	4	E2F6
Up	*CD247*	4	hsa-mir-346	Up	*BTK*	2	SOX5
Up	*MAP1LC3C*	2	hsa-mir-27a-3p	Up	*CCR5*	1	EGR1
Down	*JUN*	144	hsa-mir-3943	Down	*ATF3*	19	TP53
Down	*EGR1*	132	hsa-mir-548e-3p	Down	*EGR1*	16	ARID3A
Down	*ZFP36*	130	hsa-mir-6077	Down	*JUNB*	15	SRF
Down	*FOS*	105	hsa-mir-5586-5p	Down	*FOS*	13	CREB1
Down	*DUSP1*	97	hsa-mir-4458	Down	*PTPRO*	12	NR3C1
Down	*JUNB*	85	hsa-mir-3065-5p	Down	*NR0B2*	11	USF1
Down	*MME*	54	hsa-mir-922	Down	*MME*	9	BRCA1
Down	*NR4A2*	50	hsa-mir-29b-2-5p	Down	*JUN*	9	SP1
Down	*ATF3*	48	hsa-mir-5000-5p	Down	*DUSP1*	9	STAT3
Down	*NR4A1*	43	hsa-mir-107	Down	*NR4A1*	9	HINFP
Down	*PCK1*	38	hsa-mir-1185-1-3p	Down	*NR4A2*	7	NR2E3
Down	*PTPRO*	18	hsa-mir-203a-3p	Down	*PCK1*	6	NR2F1
Down	*APOB*	17	hsa-mir-548p	Down	*ZFP36*	5	TFAP2C
Down	*ALB*	10	hsa-mir-492	Down	*APOB*	4	FOXA1
Down	*NR0B2*	5	hsa-mir-141-3p	Down	*ALB*	4	STAT1

reported to be expressed in breast cancer. *MAP1B*[45] has been reported to be associated with lung cancer progression. BCL2 interacting protein 3 like (*BNIP3L*)[46] is involved in the progression of breast and ovarian cancer. Integrin subunit alpha 4 (*ITGA4*)[47] was found to promote oral cancer. Serine/arginine repetitive matrix 2 (*SRRM2*)[48] plays an important role in regulating thyroid carcinoma. Interleukin 7 receptor (*IL7R*)[49] plays important roles in the progression of esophageal squamous cell carcinoma. Major histocompatibility complex, class II, and DR alpha (*HLA-DRA*)[50] have been reported to encourage the development of colorectal cancer. Sestrin 3 (*SESN3*)[51] is important in the development of hepatocellular carcinoma. These genes served as biomarkers for cancer diagnosis and prognosis.

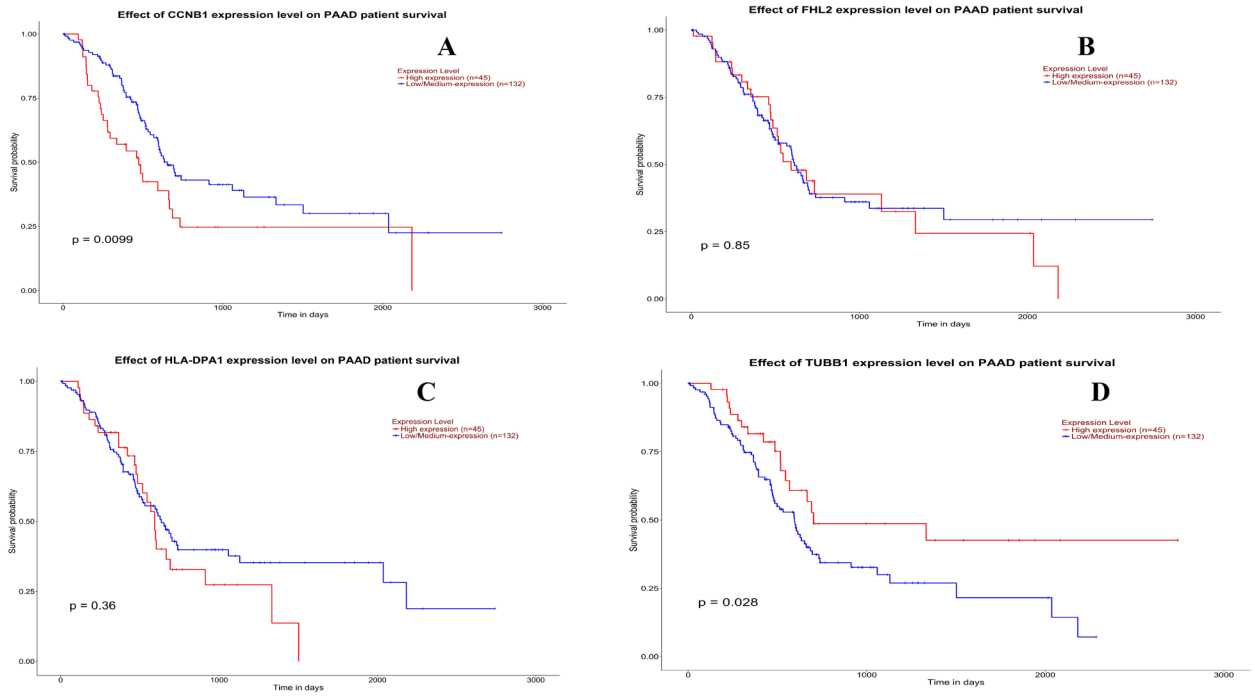

Figure 5. Overall survival analysis of hub genes. Overall survival analyses were performed using the UALCAN online platform. Red line denotes high expression; Blue line denotes low expression. (A) *CCNB1*, (B) *FHL2*, (C) *HLA-DPA1*, (D) *TUBB1*.

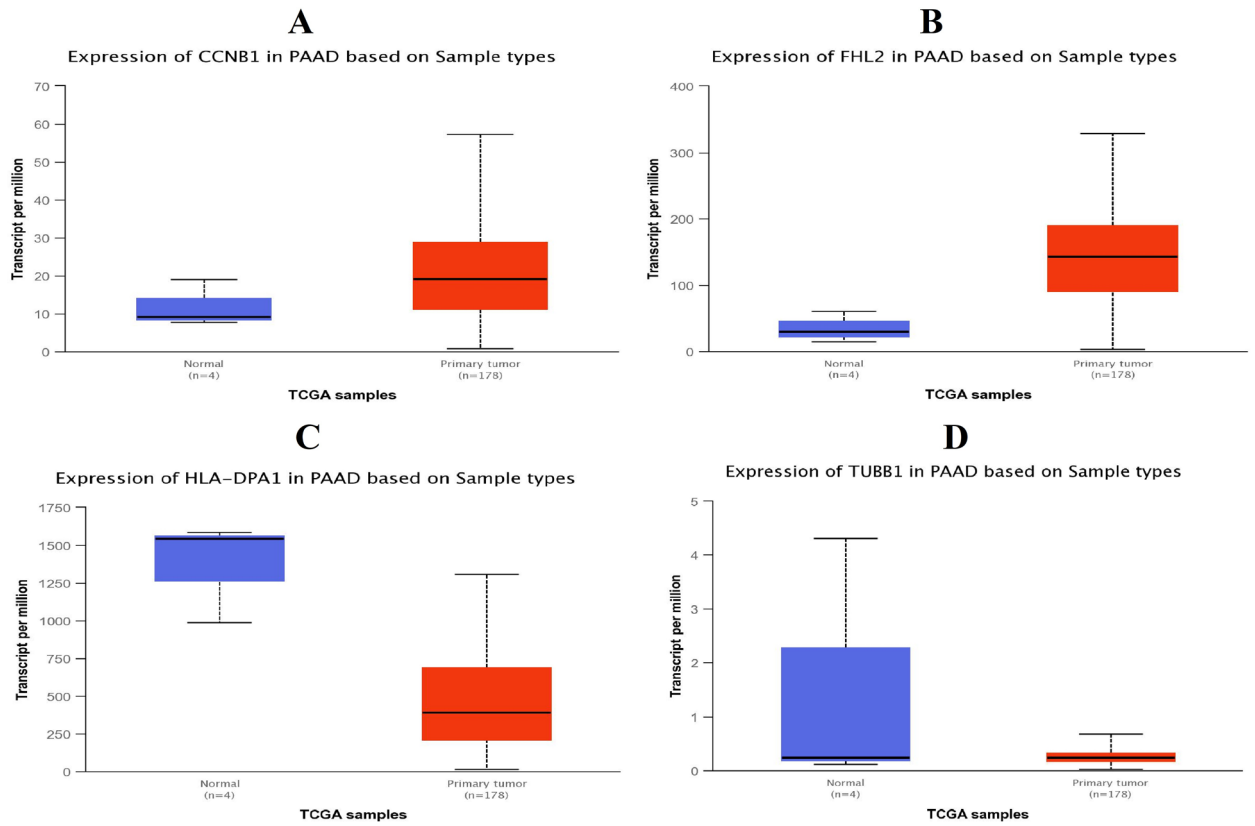

Figure 6. Box plots (expression analysis) hub genes were produced using the UALCAN platform. (A) *CCNB1*, (B) *FHL2*, (C) *HLA-DPA1*, (D) *TUBB1*.

Then, GO and REACTOME pathway analyses were used to investigate the interactions of these DEGs. Lysosomal protein transmembrane 4 beta (*LAPTM4B*),[52] CEA cell adhesion molecule 6 (*CEACAM6*),[53] serpin family E member 2 (*SERPINE2*),[54] vanin 1 (*VNN1*),[55] sphingosine kinase 1 (*SPHK1*),[56] histidine rich glycoprotein (*HRG*),[57] vascular

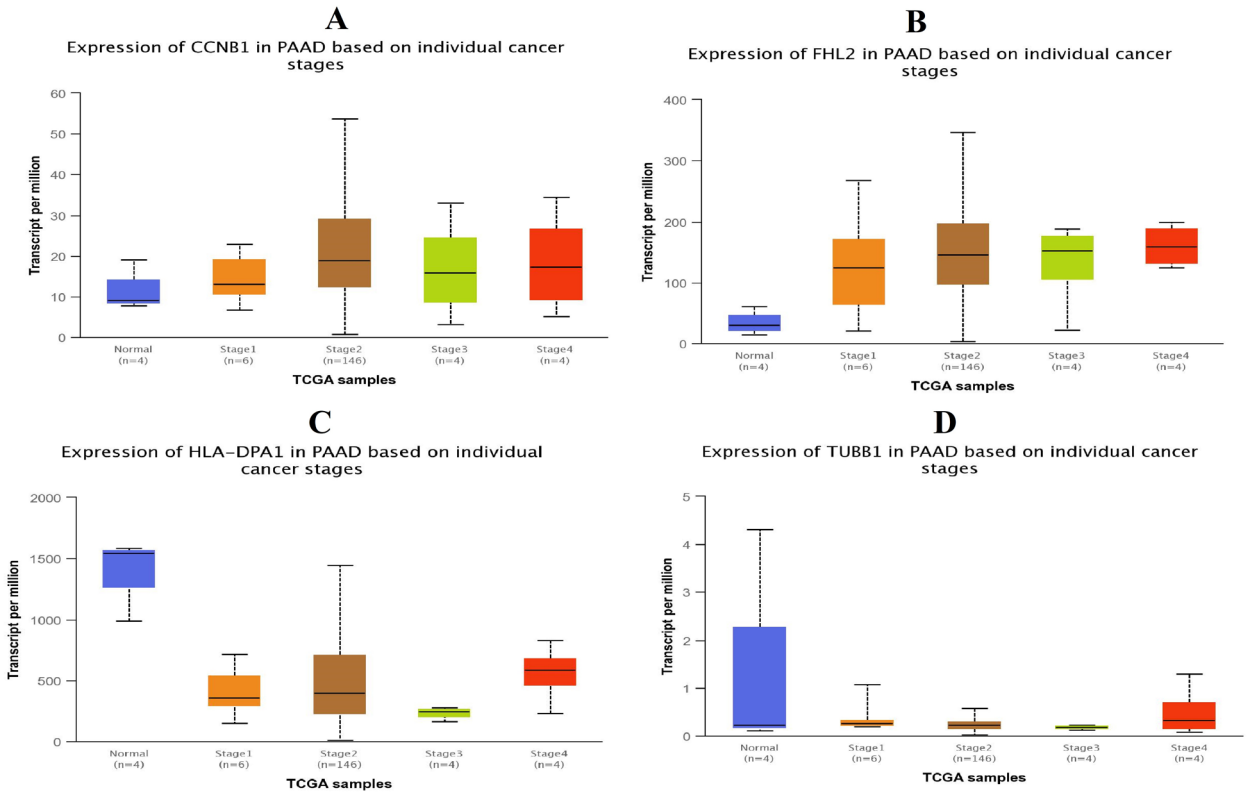

Figure 7. Box plots (clinical stage analysis) hub genes were produced using the UALCAN platform. (A) *CCNB1*, (B) *FHL2*, (C) *HLA-DPA1*, (D) *TUBB1*.

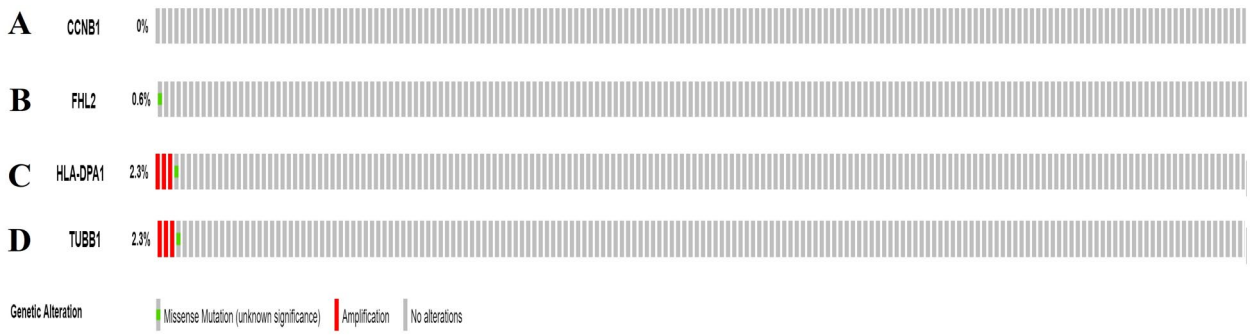

Figure 8. Mutation analyses of hub genes were produced using the CbioPortal online platform. (A) *CCNB1*, (B) *FHL2*, (C) *HLA-DPA1*, (D) *TUBB1*.

endothelial growth factor C (*VEGFC*),[58] annexin A3 (*ANXA3*),[59] apolipoprotein A2 (*APOA2*),[60] lipocalin 2 (*LCN2*),[61] TIMP metallopeptidase inhibitor 1 (*TIMP1*),[62] CD63 molecule (*CD63*),[63] CD151 molecule (Raph blood group) (*CD151*),[64] mal, T-cell differentiation protein 2 (*MAL2*),[65] aryl hydrocarbon receptor nuclear translocator-like 2 (*ARNTL2*),[66] polycystin 2, transient receptor potential cation channel (*PKD2*),[67] E2F transcription factor 1 (*E2F1*),[68] matrix metallopeptidase 1 (*MMP1*),[69] C-C motif chemokine receptor 7 (*CCR7*),[70] notch receptor 2 (*NOTCH2*),[71] B and T lymphocyte associated (*BTLA*),[72] transferrin receptor (*TFRC*),[73] CD4 molecule (*CD4*),[74] ATM serine/threonine kinase (*ATM*),[75] lymphoid enhancer binding factor 1 (*LEF1*),[76] colony stimulating factor 1 receptor (*CSF1R*),[77] cathepsin B (*CTSB*),[78] dual specificity phosphatase 2 (*DUSP2*),[79] and nuclear receptor subfamily 4 group A member 1 (*NR4A1*)[80] are pathogenic genes for PDAC. Prostaglandin E receptor 3 (*PTGER3*)[81] and membrane associated guanylate kinase, WW and PDZ domain containing 2 (*MAGI2*)[82] have been reported to encourage the development of angiogenesis, chemoresistance, cell proliferation, and migration in ovary cancer. Recent studies have proposed that the haptoglobin (*HP*)[83] is associated with progression of lung cancer. *FGA*[84] is a gene which plays a role in diagnosis of lung cancer. *FGB*[85] has been known to be involved in gastric carcinoma. Phospholipase A2 group IVA (*PLA2G4A*),[86] *FGG*,[87] thymidylatesynthetase (*TYMS*),[88] *RAB32*,[89] *SEPTIN4*,[90] *TPM2*,[91] acyl-CoA thioesterase 7 *ACOT7*,[92] phosphoribosyl transferase domain containing 1 (*PRTFDC1*),[93] Cdk5 and Abl enzyme substrate 1 (*CABLES1*),[94] major histocompatibility complex, class II, DM beta (*HLA-DMB*),[95]

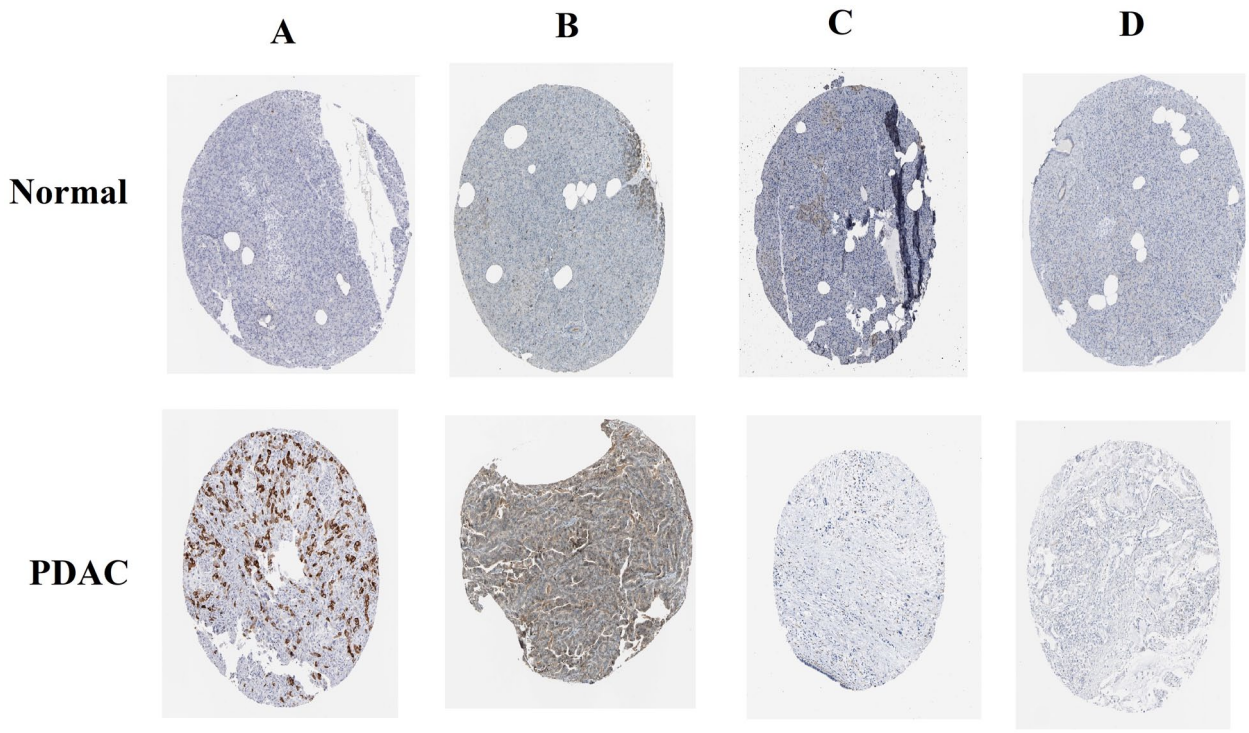

Figure 9. Immunohistochemical (IHC) analyses of hub genes were produced using the human protein atlas (HPA) online platform. (A) *CCNB1*, (B) *FHL2*, (C) *HLA-DPA1*, (D) *TUBB1*. PDAC indicates pancreatic ductal adenocarcinoma.

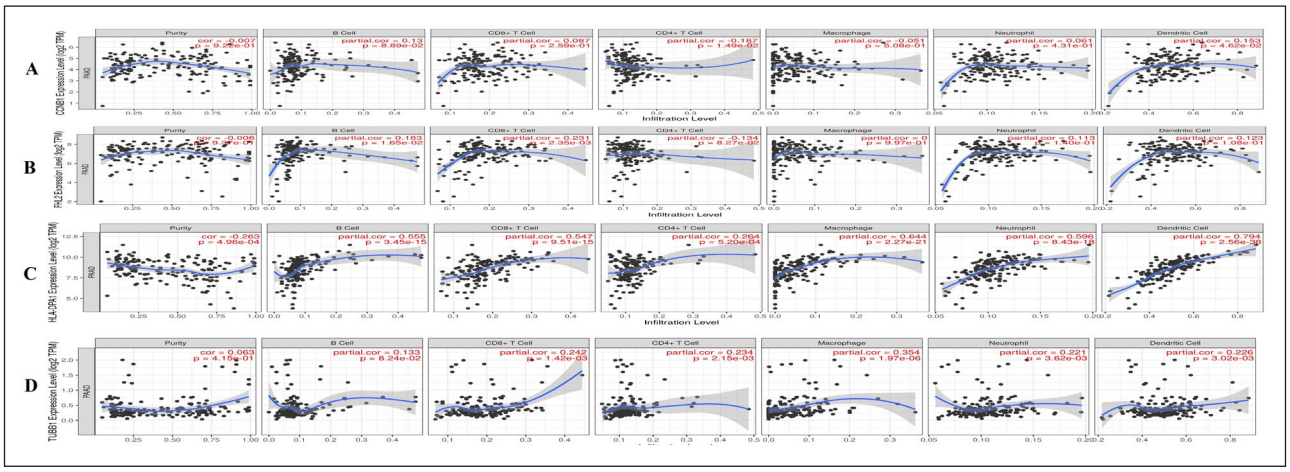

Figure 10. Scatter plot for immune infiltration for hub genes. (A) *CCNB1*, (B) *FHL2*, (C) *HLA-DPA1*, (D) *TUBB1*.

protein tyrosine phosphatase receptor type C (*PTPRC*),[96] CD5 molecule (*CD5*),[97] CD6 molecule (*CD6*),[97] membrane spanning 4-domains A1 (*MS4A1*),[98] CD22 molecule (*CD22*),[99] CD27 molecule (*CD27*),[100] mannose receptor C type 2 (*MRC2*),[101] C-type lectin domain family 2 member D (*CLEC2D*),[102] EEF1A1,[103] and apolipoprotein B (*APOB*)[104] have a significant prognostic potential in various types of cancer. Sphingomyelin phosphodiesterase 1 (*SMPD1*)[105] expression in colorectal cancer results in drug resistance. Peptidyl arginine deiminase 4 (*PADI4*),[106] monoamine oxidase B (*MAOB*),[107] transient receptor potential cation channel subfamily C member 6 (*TRPC6*),[108] BCL11 transcription factor A (*BCL11A*),[109] C-X-C motif chemokine receptor 5 (*CXCR5*),[110] transcription factor 7 (*TCF7*),[111] POU class 2 homeobox 2 (*POU2F2*),[112] solute carrier family 4 member 1 (Diego blood group) (*SLC4A1*),[113] serine/threonine kinase 17b (*STK17B*),[114] and LDL receptor-related protein 1 (*LRP1*)[115] play crucial role in cancer cell invasion. Growth factor receptor bound protein 14 (*GRB14*),[116] transient receptor potential cation channel subfamily C member 6 (*TRPC6*),[117] zinc finger protein, FOG family member 2 (*ZFPM2*),[118] TNF receptor superfamily member 13B (*TNFRSF13B*),[119] ADAM metallopeptidase domain 19 (*ADAM19*),[120] and phosphoinositide-3-kinase interacting protein 1 (*PIK3IP1*)[121] are associated with cancer cell proliferation. *HLA-DPA1*,[122] fibrinogen like 2 (*FGL2*),[123] Cbl proto-oncogene B (*CBLB*),[124] NCK associated protein 1

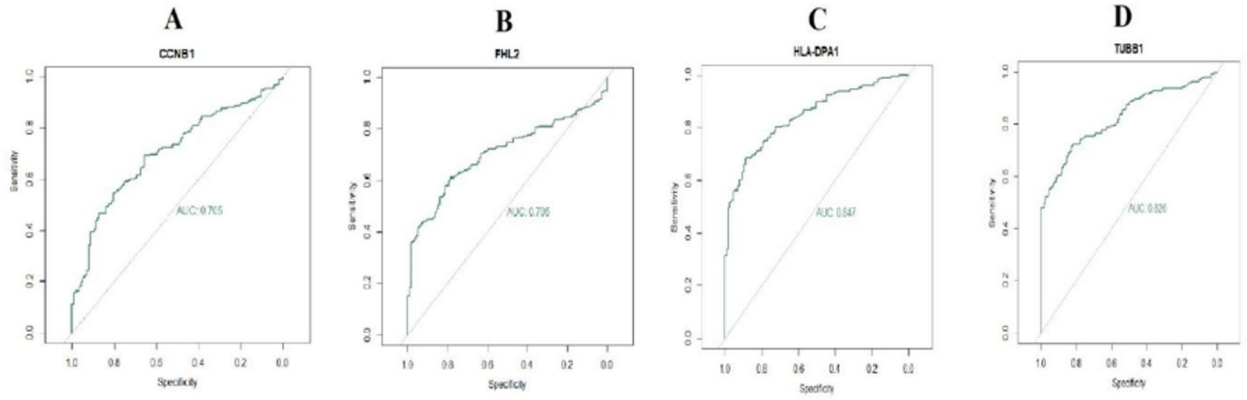

Figure 11. ROC curve validated the sensitivity and specificity of hub genes as a predictive biomarker for PDAC prognosis. (A) *CCNB1*, (B) *FHL2*, (C) *HLA-DPA1*, and (D) *TUBB1*. PDAC indicates pancreatic ductal adenocarcinoma; ROC, receiver operating characteristic.

like (*NCKAP1L*),[125] dual specificity tyrosine phosphorylation regulated kinase 2 (*DYRK2*),[126] O-linked N-acetylglucosamine (GlcNAc) transferase (*OGT*),[127] calcium-/calmodulin-dependent protein kinase ID (*CAMK1D*),[128] and ring finger protein 213 (*RNF213*)[129] are molecular markers for the diagnosis and prognosis of various types of cancer. Recent reports have revealed that RAR-related orphan receptor A (RORA),[130] insulin-like growth factor 2 receptor (IGF2R),[131] and zinc finger and BTB domain containing 20 (*ZBTB20*)[132] acted as polymorphic genes in various types of cancer. Versican (*VCAN*)[133] induces immune cell infiltration in cancer. Therefore, these enriched GO and pathways are most likely to be essential in the development of PDAC. In the future investigation, we might combine gene expression levels of these enriched genes and cell biological behavior analysis to further explore the pathogenesis of PDAC.

To explore the molecular mechanism of PDAC, we constructed the PDAC-related PPI network. CCNB1[134] plays a crucial role in proliferation of cancer cells. Recent reports have revealed that FHL2[135] and RPL10[136] acted as genetic factors in PDAC. FGB,[85] FGA,[84] FGG,[87] eukaryotic translation elongation factor 1 alpha 1 (EEF1A1),[103] and integrin subunit alpha 4 (ITGA4)[47] might be diagnostic markers of cancer and could be used as therapeutic targets. HLA-DPA1, TUBB1, RPL13A, RPL27A, and RPL23A were the novel potential gene targets of the drugs for treating PDAC in this investigation. Importantly, study on ribosomal proteins might be a significant novel direction for the diagnosis, prognosis, and treatment of PDAC.

The miRNA-DEG regulatory network and TF-DEG regulatory network were constructed to explore the molecular mechanism of PDAC. Researchers have shown that AHNAK[41], E2F transcription factor 1 (E2F1),[68] cathepsin B (CTSB),[78] O-linked N-acetylglucosamine (GlcNAc) transferase (OGT),[127] FHL2,[135] EZH2,[137] KMT2D,[138] TXNIP,[139] TP63,[140] SOX2,[141] MYC,[142] and KLF4[143] promoted PDAC. MAP1B,[45] CCNB1,[134] TPM1,[144] and hsa-mir-1202[145] might be novel prognostic markers of cancer. We identified SEC16 homolog A, endoplasmic reticulum export factor (SEC16A), keratin 18 (KRT18), period circadian regulator 1 (PER1), hsa-mir-4461, hsa-mir-3928-3p, and hsa-mir-2682-5p might serve as potential novel biomarkers for PDAC. Therefore, these biomarkers might be used as potential effective candidates for early diagnosis or prognosis of PDAC.

Bioinformatics analysis has been performed and NGS data analysis has been carried out in these present investigations, but limitations exist. Lack of experimental validation of the hub genes is a limitation of the investigation. Corresponding experiments will be performed to verify hub genes in our future work, thus conversely testifying in bioinformatics analysis.

In conclusion, using NGS data set and integrated bioinformatics analysis, PDAC-associated hub genes were identified. The expression of the hub genes was revealed to be altered in PDAC. Experimental evidence is warranted to investigate the functional roles of the identified hub genes in PDAC. Collectively, it is our sincere hope that the present investigations will contribute to the discovery of new diagnostic and prognostic biomarkers as well as therapeutic targets for PDAC.

Acknowledgements

I thank Shenglin Huang, Fudan University, Shanghai, China, very much, the author who deposited their NGS data set, GSE133684, into the public GEO database.

Author Contributions

Muttanagouda Giriyappagoudar—Acquisition of resources and investigation.Basavaraj Vastrad—Writing original draft, and review and editing.Rajeshwari Horakeri—Formal analysis and validation.Chanabasayya Vastrad—Software and investigation.

Ethical Approval

This article does not contain any studies with human participants or animals performed by any of the authors.

Informed Consent

No informed consent because this study does not contain human or animals participants.

Consent for Publication

Not applicable.

Availability of Data and Materials

The data sets supporting the conclusions of this article are available in the GEO (Gene Expression Omnibus) (https://www.ncbi.nlm.nih.gov/geo/) repository ([GSE133684] [https://www.ncbi.nlm.nih.gov/geo/query/acc.cgi?acc=GSE133684]).

REFERENCES

1. Thiruvengadam SS, Chuang J, Huang R, Girotra M, Park WG. Chronic pancreatitis changes in high-risk individuals for pancreatic ductal adenocarcinoma. *Gastrointest Endosc*. 2019;89:842-851. doi:10.1016/j.gie.2018.08.029
2. McGuigan A, Kelly P, Turkington RC, Jones C, Coleman HG, McCain RS. Pancreatic cancer: a review of clinical diagnosis, epidemiology, treatment and outcomes. *World J Gastroenterol*. 2018;24:4846-4861. doi:10.3748/wjg.v24.i43.4846
3. Al-Hawary MM, Kaza RK, Azar SF, Ruma JA, Francis IR. Mimics of pancreatic ductal adenocarcinoma. *Cancer Imag*. 2013;13:342-349. doi:10.1102/1470-7330.2013.9012
4. Siegel RL, Miller KD, Jemal A. Cancer statistics, 2018. *CA. Cancer J Clin*. 2018;68:7-30. doi:10.3322/caac.21442
5. Campello E, Bosch F, Simion C, Spiezia L, Simioni P. Mechanisms of thrombosis in pancreatic ductal adenocarcinoma. *Best Pract Res Clin Haematol*. 2022;35:101346. doi:10.1016/j.beha.2022.101346
6. Schizas D, Charalampakis N, Kole C, et al. Immunotherapy for pancreatic cancer: a 2020 update. *Cancer Treat Rev*. 2020;86:102016. doi:10.1016/j.ctrv.2020.102016
7. Adamska A, Domenichini A, Falasca M. Pancreatic ductal adenocarcinoma: current and evolving therapies. *Int J Mol Sci*. 2017;18:1338. doi:10.3390/ijms18071338
8. Tsuchiya N, Matsuyama R, Murakami T, et al. Risk factors associated with early recurrence of borderline resectable pancreatic ductal adenocarcinoma after neoadjuvant chemoradiation therapy and curative resection. *Anticancer Res*. 2019;39:4431-4440. doi:10.21873/anticanres.13615
9. Vitone LJ, Greenhalf W, McFaul CD, Ghaneh P, Neoptolemos JP. The inherited genetics of pancreatic cancer and prospects for secondary screening. *Best Pract Res Clin Gastroenterol*. 2006;20:253-283. doi:10.1016/j.bpg.2005.10.007
10. Oji Y, Nakamori S, Fujikawa M, et al. Overexpression of the Wilms' tumor gene WT1 in pancreatic ductal adenocarcinoma. *Cancer Sci*. 2004;95:583-587. doi:10.1111/j.1349-7006.2004.tb02490.x
11. Murthy D, Attri KS, Singh PK. Phosphoinositide 3-kinase signaling pathway in pancreatic ductal adenocarcinoma progression, pathogenesis, and therapeutics. *Front Physiol*. 2018;9:335. doi:10.3389/fphys.2018.00335
12. Reddy RRS, Ramanujam MV. High throughput sequencing-based approaches for gene expression analysis. *Methods Mol Biol*. 2018;1783:299-323. doi:10.1007/978-1-4939-7834-2_15
13. Gu Y, Feng Q, Liu H, et al. Bioinformatic evidences and analysis of putative biomarkers in pancreatic ductal adenocarcinoma. *Heliyon*. 2019;5:e02378. doi:10.1016/j.heliyon.2019.e02378
14. Clough E, Barrett T. The gene expression omnibus database. *Methods Mol Biol*. 2016;1418:93-110. doi:10.1007/978-1-4939-3578-9_5
15. Yu S, Li Y, Liao Z, et al. Plasma extracellular vesicle long RNA profiling identifies a diagnostic signature for the detection of pancreatic ductal adenocarcinoma. *Gut*. 2020;69:540-550. doi:10.1136/gutjnl-2019-318860
16. Ritchie ME, Phipson B, Wu D, et al. Limma powers differential expression analyses for RNA-sequencing and microarray studies. *Nucleic Acids Res*. 2015;43:e47. doi:10.1093/nar/gkv007
17. Ferreira JA. The Benjamini-Hochberg method in the case of discrete test statistics. *Int J Biostat*. 2007;3:Article 11. doi:10.2202/1557-4679.1065
18. Thomas PD. The gene ontology and the meaning of biological function. *Methods Mol Biol*. 2017;1446:15-24. doi:10.1007/978-1-4939-3743-1_2
19. Fabregat A, Jupe S, Matthews L, et al. The reactome pathway knowledgebase. *Nucleic Acids Res*. 2018;46:D649-D655. doi:10.1093/nar/gkx1132
20. Chen J, Bardes EE, Aronow BJ, Jegga AG. ToppGene Suite for gene list enrichment analysis and candidate gene prioritization. *Nucleic Acids Res*. 2009;37:W305-W311. doi:10.1093/nar/gkp427
21. Kotlyar M, Pastrello C, Malik Z, Jurisica I. IID 2018 update: context-specific physical protein-protein interactions in human, model organisms and domesticated species. *Nucleic Acids Res*. 2019;47:D581-D589. doi:10.1093/nar/gky1037
22. Shannon P, Markiel A, Ozier O, et al. Cytoscape: a software environment for integrated models of biomolecular interaction networks. *Genome Res*. 2003;13:2498-2504. doi:10.1101/gr.1239303
23. Przulj N, Wigle DA, Jurisica I. Functional topology in a network of protein interactions. *Bioinformatics*. 2004;20:340-348. doi:10.1093/bioinformatics/btg415
24. Nguyen TP, Liu WC, Jordán F. Inferring pleiotropy by network analysis: linked diseases in the human PPI network. *BMC Syst Biol*. 2011;5:179. doi:10.1186/1752-0509-5-179
25. Shi Z, Zhang B. Fast network centrality analysis using GPUs. *BMC Bioinformatics*. 2011;12:149. doi:10.1186/1471-2105-12-149
26. Fadhal E, Gamieldien J, Mwambene EC. Protein interaction networks as metric spaces: a novel perspective on distribution of hubs. *BMC Syst Biol*. 2014;8:6. doi:10.1186/1752-0509-8-6
27. Zaki N, Efimov D, Berengueres J. Protein complex detection using interaction reliability assessment and weighted clustering coefficient. *BMC Bioinformatics*. 2013;14:163. doi:10.1186/1471-2105-14-163
28. Fan Y, Xia J. miRNet-functional analysis and visual exploration of miRNA-target interactions in a network context. *Methods Mol Biol*. 2018;1819:215-233. doi:10.1007/978-1-4939-8618-7_10
29. Zhou G, Soufan O, Ewald J, Hancock REW, Basu N, Xia J. NetworkAnalyst 3.0: a visual analytics platform for comprehensive gene expression profiling and meta-analysis. *Nucleic Acids Res*. 2019;47:W234-W241. doi:10.1093/nar/gkz240
30. Chandrashekar DS, Bashel B, Balasubramanya SAH, et al. UALCAN: a portal for facilitating tumor subgroup gene expression and survival analyses. *Neoplasia*. 2017;19:649-658. doi:10.1016/j.neo.2017.05.002
31. Gao J, Aksoy BA, Dogrusoz U, et al. Integrative analysis of complex cancer genomics and clinical profiles using the cBioPortal. *Sci Signal*. 2013;6:l1. doi:10.1126/scisignal.2004088
32. Uhlen M, Oksvold P, Fagerberg L, et al. Towards a knowledge-based human protein atlas. *Nat Biotechnol*. 2010;28:1248-1250. doi:10.1038/nbt1210-1248
33. Li T, Fan J, Wang B, et al. TIMER: a web server for comprehensive analysis of tumor-infiltrating immune cells. *Cancer Res*. 2017;77:e108-e110. doi:10.1158/0008-5472.CAN-17-0307
34. Robin X, Turck N, Hainard A, et al. pROC: an open-source package for R and S+ to analyze and compare ROC curves. *BMC Bioinformatics*. 2011;12:77. doi:10.1186/1471-2105-12-77
35. Moffitt RA, Marayati R, Flate EL, et al. Virtual microdissection identifies distinct tumor- and stroma-specific subtypes of pancreatic ductal adenocarcinoma. *Nat Genet*. 2015;47:1168-1178. doi:10.1038/ng.3398
36. Dansranjavin T, Möbius C, Tannapfel A, et al. E-cadherin and DAP kinase in pancreatic adenocarcinoma and corresponding lymph node metastases. *Oncol Rep*. 2006;15:1125-1131.
37. Treiber M, Schulz HU, Landt O, et al. Keratin 8 sequence variants in patients with pancreatitis and pancreatic cancer. *J Mol Med (Berl)*. 2006;84:1015-1022. doi:10.1007/s00109-006-0096-7
38. Liu H, Li L, Chen H, et al. Silencing IGFBP-2 decreases pancreatic cancer metastasis and enhances chemotherapeutic sensitivity. *Oncotarget*. 2017;8:61674-61686. doi:10.18632/oncotarget.18669
39. Yao H, Yang Z, Liu Z, et al. Glypican-3 and KRT19 are markers associating with metastasis and poor prognosis of pancreatic ductal adenocarcinoma. *Cancer Biomark*. 2016;17:397-404. doi:10.3233/CBM-160655
40. Huynh DL, Koh H, Chandimali N, et al. BRM270 inhibits the proliferation of CD44 positive pancreatic ductal adenocarcinoma cells via downregulation of sonic hedgehog signaling. *Evid Based Complement Alternat Med*. 2019;2019:8620469. doi:10.1155/2019/8620469
41. Zhang Z, Liu X, Huang R, Liu X, Liang Z, Liu T. Upregulation of nucleoprotein AHNAK is associated with poor outcome of pancreatic ductal adenocarcinoma prognosis via mediating epithelial-mesenchymal transition. *J Cancer*. 2019;10:3860-3870. doi:10.7150/jca.31291
42. Huang Y, Zheng J, Tan T, et al. BTG1 low expression in pancreatic ductal adenocarcinoma is associated with a poorer prognosis. *Int J Biol Markers*. 2018;33:189-194. doi:10.5301/ijbm.5000310
43. Wang PB, Chen Y, Ding GR, Du HW, Fan HY. Keratin 18 induces proliferation, migration, and invasion in gastric cancer via the MAPK signalling pathway [published online ahead of print August 28, 2020]. *Clin Exp Pharmacol Physiol*. doi:10.1111/1440-1681.13401
44. Alfarsi LH, El Ansari R, Masisi BK, et al. Integrated analysis of key differentially expressed genes identifies DBN1 as a predictive marker of response to endocrine therapy in luminal breast cancer. *Cancers (Basel)*. 2020;12:1549. doi:10.3390/cancers12061549
45. Tessema M, Yingling CM, Picchi MA, et al. Epigenetic repression of CCDC37 and MAP1B links chronic obstructive pulmonary disease to lung cancer. *J Thorac Oncol*. 2015;10:1181-1188. doi:10.1097/JTO.0000000000000592
46. Lai J, Flanagan J, Phillips WA, Chenevix-Trench G, Arnold J. Analysis of the candidate 8p21 tumour suppressor, BNIP3L, in breast and ovarian cancer. *Br J Cancer*. 2003;88:270-276. doi:10.1038/sj.bjc.6600674

47. Yen CY, Huang CY, Hou MF, et al. Evaluating the performance of fibronectin 1 (FN1), integrin α4β1 (ITGA4), syndecan-2 (SDC2), and glycoprotein CD44 as the potential biomarkers of oral squamous cell carcinoma (OSCC). *Biomarkers*. 2013;18:63-72. doi:10.3109/1354750X.2012.737025
48. Tomsic J, He H, Akagi K, et al. A germline mutation in SRRM2, a splicing factor gene, is implicated in papillary thyroid carcinoma predisposition. *Sci Rep*. 2015;5:10566. doi:10.1038/srep10566
49. Kim MJ, Choi SK, Hong SH, et al. Oncogenic IL7R is downregulated by histone deacetylase inhibitor in esophageal squamous cell carcinoma via modulation of acetylated FOXO1. *Int J Oncol*. 2018;53:395-403. doi:10.3892/ijo.2018.4392
50. Lee J, Li L, Gretz N, Gebert J, Dihlmann S. Absent in Melanoma 2 (AIM2) is an important mediator of interferon-dependent and -independent HLA-DRA and HLA-DRB gene expression in colorectal cancers. *Oncogene*. 2012;31:1242-1253. doi:10.1038/onc.2011.320
51. Liu Y, Kim HG, Dong E, et al. Sesn3 deficiency promotes carcinogen-induced hepatocellular carcinoma via regulation of the hedgehog pathway. *Biochim Biophys Acta Mol Basis Dis*. 2019;1865:2685-2693. doi:10.1016/j.bbadis.2019.07.011
52. Yang Z, Senninger N, Flammang I, Ye Q, Dhayat SA. Clinical impact of circulating LAPTM4B-35 in pancreatic ductal adenocarcinoma. *J Cancer Res Clin Oncol*. 2019;145:1165-1178. doi:10.1007/s00432-019-02863-w
53. Pandey R, Zhou M, Islam S, et al. Carcinoembryonic antigen cell adhesion molecule 6 (CEACAM6) in pancreatic ductal adenocarcinoma (PDA): an integrative analysis of a novel therapeutic target. *Sci Rep*. 2019;9:18347. doi:10.1038/s41598-019-54545-9
54. Neesse A, Wagner M, Ellenrieder V, Bachem M, Gress TM, Buchholz M. Pancreatic stellate cells potentiate proinvasive effects of SERPINE2 expression in pancreatic cancer xenograft tumors. *Pancreatology*. 2007;7:380-385. doi:10.1159/000107400
55. Kang M, Qin W, Buya M, et al. VNN1, a potential biomarker for pancreatic cancer-associated new-onset diabetes, aggravates paraneoplastic islet dysfunction by increasing oxidative stress. *Cancer Lett*. 2016;373:241-250. doi:10.1016/j.canlet.2015.12.031
56. Li J, Wu H, Li W, et al. Downregulated miR-506 expression facilitates pancreatic cancer progression and chemoresistance via SPHK1/Akt/NF-κB signaling. *Oncogene*. 2016;35:5501-5514. doi:10.1038/onc.2016.90
57. Chen XL, Xie KX, Yang ZL, Yuan LW. Expression of FXR and HRG and their clinicopathological significance in benign and malignant pancreatic lesions. *Int J Clin Exp Pathol*. 2019;12:2111-2120.
58. Guo J, Lou W, Ji Y, Zhang S. Effect of CCR7, CXCR4 and VEGF-C on the lymph node metastasis of human pancreatic ductal adenocarcinoma. *Oncol Lett*. 2013;5:1572-1578. doi:10.3892/ol.2013.1261
59. Wan YCE, Liu J, Zhu L, et al. The H2BG53D oncohistone directly upregulates ANXA3 transcription and enhances cell migration in pancreatic ductal adenocarcinoma. *Signal Transduct Target Ther*. 2020;5:106. doi:10.1038/s41392-020-00219-2
60. Sato Y, Kobayashi T, Nishiumi S, et al. Prospective study using plasma apolipoprotein A2-isoforms to screen for high-risk status of pancreatic cancer. *Cancers (Basel)*. 2020;12:E2625. doi:10.3390/cancers12092625
61. Gumpper K, Dangel AW, Pita-Grisanti V, et al. Lipocalin-2 expression and function in pancreatic diseases. *Pancreatology*. 2020;20:419-424. doi:10.1016/j.pan.2020.01.002
62. D' Costa Z, Jones K, Azad A, et al. Gemcitabine-induced TIMP1 attenuates therapy response and promotes tumor growth and liver metastasis in pancreatic cancer. *Cancer Res*. 2017;77:5952-5962. doi:10.1158/0008-5472.CAN-16-2833
63. Buscail E, Chauvet A, Quincy P, et al. CD63-GPC1-positive exosomes coupled with CA19-9 offer good diagnostic potential for resectable pancreatic ductal adenocarcinoma. *Transl Oncol*. 2019;12:1395-1403. doi:10.1016/j.tranon.2019.07.009
64. Zhu GH, Huang C, Qiu ZJ, et al. Expression and prognostic significance of CD151, c-Met, and integrin alpha3/alpha6 in pancreatic ductal adenocarcinoma. *Dig Dis Sci*. 2011;56:1090-1098. doi:10.1007/s10620-010-1416-x
65. Eguchi D, Ohuchida K, Kozono S, et al. MAL2 expression predicts distant metastasis and short survival in pancreatic cancer. *Surgery*. 2013;154:573-582. doi:10.1016/j.surg.2013.03.010
66. Wang Z, Liu T, Xue W, et al. ARNTL2 promotes pancreatic ductal adenocarcinoma progression through TGF/BETA pathway and is regulated by miR-26a-5p. *Cell Death Dis*. 2020;11:692. doi:10.1038/s41419-020-02839-6
67. Yuan J, Rozengurt E. PKD, PKD2, and p38 MAPK mediate Hsp27 serine-82 phosphorylation induced by neurotensin in pancreatic cancer PANC-1 cells. *J Cell Biochem*. 2008;103:648-662. doi:10.1002/jcb.21439
68. Schild C, Wirth M, Reichert M, Schmid RM, Saur D, Schneider G. PI3K signaling maintains c-myc expression to regulate transcription of E2F1 in pancreatic cancer cells. *Mol Carcinog*. 2009;48:1149-1158. doi:10.1002/mc.2056
69. Chen Y, Peng S, Cen H, et al. MicroRNA hsa-miR-623 directly suppresses MMP1 and attenuates IL-8-induced metastasis in pancreatic cancer. *Int J Oncol*. 2019;55:142-156. doi:10.3892/ijo.2019.4803
70. Wang L, Zhao XY, Zhu JS, et al. CCR7 regulates ANO6 to promote migration of pancreatic ductal adenocarcinoma cells via the ERK signaling pathway. *Oncol Lett*. 2018;16:2599-2605. doi:10.3892/ol.2018.8962
71. Mazur PK, Einwächter H, Lee M, et al. Notch2 is required for progression of pancreatic intraepithelial neoplasia and development of pancreatic ductal adenocarcinoma. *Proc Natl Acad Sci USA*. 2010;107:13438-13443. doi:10.1073/pnas.1002423107
72. Bian B, Fanale D, Dusetti N, et al. Prognostic significance of circulating PD-1, PD-L1, pan-BTN3As, BTN3A1 and BTLA in patients with pancreatic adenocarcinoma. *Oncoimmunology*. 2019;8:e1561120. doi:10.1080/2162402X.2018.1561120
73. Ryschich E, Huszty G, Knaebel HP, Hartel M, Büchler MW, Schmidt J. Transferrin receptor is a marker of malignant phenotype in human pancreatic cancer and in neuroendocrine carcinoma of the pancreas. *Eur J Cancer*. 2004;40:1418-1422. doi:10.1016/j.ejca.2004.01.036
74. Sonntag K, Hashimoto H, Eyrich M, et al. Immune monitoring and TCR sequencing of CD4 T cells in a long term responsive patient with metastasized pancreatic ductal carcinoma treated with individualized, neoepitope-derived multipeptide vaccines: a case report. *J Transl Med*. 2018;16:23. doi:10.1186/s12967-018-1382-1
75. Hutchings D, Jiang Z, Skaro M, et al. Histomorphology of pancreatic cancer in patients with inherited ATM—serine/threonine kinase pathogenic variants. *Mod Pathol*. 2019;32:1806-1813. doi:10.1038/s41379-019-0317-6
76. Singhi AD, Lilo M, Hruban RH, Cressman KL, Fuhrer K, Seethala RR. Overexpression of lymphoid enhancer-binding factor 1 (LEF1) in solid-pseudopapillary neoplasms of the pancreas. *Mod Pathol*. 2014;27:1355-1363. doi:10.1038/modpathol.2014.40
77. Zhu Y, Knolhoff BL, Meyer MA, et al. CSF1/CSF1R blockade reprograms tumor-infiltrating macrophages and improves response to T-cell checkpoint immunotherapy in pancreatic cancer models. *Cancer Res*. 2014;74:5057-5069. doi:10.1158/0008-5472.CAN-13-3723
78. Dumartin L, Whiteman HJ, Weeks ME, et al. AGR2 is a novel surface antigen that promotes the dissemination of pancreatic cancer cells through regulation of cathepsins B and D. *Cancer Res*. 2011;71:7091–7102. doi:10.1158/0008-5472.CAN-11-1367
79. Wang CA, Chang IH, Hou PC, et al. DUSP2 regulates extracellular vesicle-VEGF-C secretion and pancreatic cancer early dissemination. *J Extracell Vesicles*. 2020;9:1746529. doi:10.1080/20013078.2020.1746529
80. Yoon K, Lee SO, Cho SD, Kim K, Khan S, Safe S. Activation of nuclear TR3 (NR4A1) by a diindolylmethane analog induces apoptosis and proapoptotic genes in pancreatic cancer cells and tumors. *Carcinogenesis*. 2011;32:836-842. doi:10.1093/carcin/bgr040
81. Rodriguez-Aguayo C, Bayraktar E, Ivan C, et al. PTGER3 induces ovary tumorigenesis and confers resistance to cisplatin therapy through up-regulation Ras-MAPK/Erk-ETS1-ELK1/CFTR1 axis. eBioMedicine. 2019;40:290-304. doi:10.1016/j.ebiom.2018.11.045
82. Chang H, Zhang X, Li B, Meng X. MAGI2-AS3 suppresses MYC signaling to inhibit cell proliferation and migration in ovarian cancer through targeting miR-525-5p/MXD1 axis. *Cancer Med*. 2020;9:6377-6386. doi:10.1002/cam4.3126
83. Hoagland LF, Campa MJ, Gottlin EB, Herndon JE, Patz EF. Haptoglobin and posttranslational glycan-modified derivatives as serum biomarkers for the diagnosis of nonsmall cell lung cancer. *Cancer*. 2007;110:2260-2268. doi:10.1002/cncr.23049
84. Wang M, Zhang G, Zhang Y, et al. Fibrinogen alpha chain knockout promotes tumor growth and metastasis through integrin-AKT signaling pathway in lung cancer. *Mol Cancer Res*. 2020;18:943-954. doi:10.1158/1541-7786.MCR-19-1033
85. Repetto O, Maiero S, Magris R, et al. Quantitative proteomic approach targeted to fibrinogen β chain in tissue gastric carcinoma. *Int J Mol Sci*. 2018;19:759. doi:10.3390/ijms19030759
86. Bazhan D, Khaniani MS. Supplementation with omega fatty acids increases the mRNA expression level of PLA2G4A in patients with gastric cancer. *J Gastrointest Oncol*. 2018;9:1176-1183. doi:10.21037/jgo.2018.08.12
87. Duan S, Gong B, Wang P, Huang H, Luo L, Liu F. Novel prognostic biomarkers of gastric cancer based on gene expression microarray: COL12A1, GSTA3, FGA and FGG. *Mol Med Rep*. 2018;18:3727-3736. doi:10.3892/mmr.2018.9368
88. Lee SW, Chen TJ, Lin LC, et al. Overexpression of thymidylate synthetase confers an independent prognostic indicator in nasopharyngeal carcinoma. Exp Mol Pathol. 2013;95:83-90. doi:10.1016/j.yexmp.2013.05.006
89. Shibata D, Mori Y, Cai K, et al. RAB32 hypermethylation and microsatellite instability in gastric and endometrial adenocarcinomas. *Int J Cancer*. 2006;119:801-806. doi:10.1002/ijc.21912
90. Zhao X, Feng H, Wang Y, et al. Septin4 promotes cell death in human colon cancer cells by interacting with BAX. *Int J Biol Sci*. 2020;16:1917-1928. doi:10.7150/ijbs.44429
91. Zhang J, Zhang J, Xu S, et al. Hypoxia-induced TPM2 methylation is associated with chemoresistance and poor prognosis in breast cancer. *Cell Physiol Biochem*. 2018;45:692-705. doi:10.1159/000487162
92. Feng H, Liu X. Interaction between ACOT7 and LncRNA NMRAL2P via methylation regulates gastric cancer progression. *Yonsei Med J*. 2020;61:471-481. doi:10.3349/ymj.2020.61.6.471

93. Suzuki E, Imoto I, Pimkhaokham A, et al. PRTFDC1, a possible tumor-suppressor gene, is frequently silenced in oral squamous-cell carcinomas by aberrant promoter hypermethylation. *Oncogene*. 2007;26:7921-7932. doi:10.1038/sj.onc.1210589
94. Sakamoto H, Friel AM, Wood AW, et al. Mechanisms of Cables 1 gene inactivation in human ovarian cancer development. *Cancer Biol Ther*. 2008;7:180-188. doi:10.4161/cbt.7.2.5253
95. Callahan MJ, Nagymanyoki Z, Bonome T, et al. Increased HLA-DMB expression in the tumor epithelium is associated with increased CTL infiltration and improved prognosis in advanced-stage serous ovarian cancer. *Clin Cancer Res*. 2008;14:7667-7673. doi:10.1158/1078-0432.CCR-08-0479
96. Wu Y, Han J, Vladimirovna KE, et al. Upregulation of protein tyrosine phosphatase receptor type C associates to the combination of Hashimoto's thyroiditis and papillary thyroid carcinoma and is predictive of a poor prognosis. *Onco Targets Ther*. 2019;12:8479-8489. doi:10.2147/OTT.S226426
97. Moreno-Manuel A, Jantus-Lewintre E, Simões I, et al. CD5 and CD6 as immunoregulatory biomarkers in non-small cell lung cancer. *Transl Lung Cancer Res*. 2020;9:1074-1083. doi:10.21037/tlcr-19-445
98. Wright CM, Savarimuthu Francis SM, Tan ME, et al. MS4A1 dysregulation in asbestos-related lung squamous cell carcinoma is due to CD20 stromal lymphocyte expression. *PLoS ONE*. 2012;7:e34943. doi:10.1371/journal.pone.0034943
99. Tuscano JM, Kato J, Pearson D, et al. CD22 antigen is broadly expressed on lung cancer cells and is a target for antibody-based therapy. *Cancer Res*. 2012;72:5556-5565. doi:10.1158/0008-5472.CAN-12-0173
100. Nielsen JS, Sahota RA, Milne K, et al. CD20+ tumor-infiltrating lymphocytes have an atypical CD27- memory phenotype and together with CD8+ T cells promote favorable prognosis in ovarian cancer. *Clin Cancer Res*. 2012;18:3281-3292. doi:10.1158/1078-0432.CCR-12-0234
101. Gai X, Tu K, Lu Z, Zheng X. MRC2 expression correlates with TGFβ1 and survival in hepatocellular carcinoma. *Int J Mol Sci*. 2014;15:15011-15025. doi:10.3390/ijms150915011
102. Mathew SO, Chaudhary P, Powers SB, Vishwanatha JK, Mathew PA. Overexpression of LLT1 (OCIL, CLEC2D) on prostate cancer cells inhibits NK cell-mediated killing through LLT1-NKRP1A (CD161) interaction. *Oncotarget*. 2016;7:68650-68661. doi:10.18632/oncotarget.11896
103. Joung EK, Kim J, Yoon N, et al. Expression of EEF1A1 is associated with prognosis of patients with colon adenocarcinoma. *J Clin Med*. 2019;8:1903. doi:10.3390/jcm8111903
104. Yang DD, Chen ZH, Wang DS, et al. Prognostic value of the serum apolipoprotein B to apolipoprotein A-I ratio in metastatic colorectal cancer patients. *J Cancer*. 2020;11:1063-1074. doi:10.7150/jca.3565
105. Jung JH, Taniguchi K, Lee HM, et al. Comparative lipidomics of 5-fluorouracil-sensitive and -resistant colorectal cancer cells reveals altered sphingomyelin and ceramide controlled by acid sphingomyelinase (SMPD1). *Sci Rep*. 2020;10:6124. doi:10.1038/s41598-020-62823-0
106. Liu M, Qu Y, Teng X, et al. PADI4-mediated epithelial-mesenchymal transition in lung cancer cells. *Mol Med Rep*. 2019;19:3087-3094. doi:10.3892/mmr.2019.9968
107. Yang YC, Chien MH, Lai TC, et al. Monoamine oxidase B expression correlates with a poor prognosis in colorectal cancer patients and is significantly associated with epithelial-to-mesenchymal transition-related gene signatures. *Int J Mol Sci*. 2020;21:2813. doi:10.3390/ijms21082813
108. Song Y, Liu G, Liu S, et al. Helicobacter pylori upregulates TRPC6 via Wnt/β-catenin signaling to promote gastric cancer migration and invasion. *Onco Targets Ther*. 2019;12:5269-5279. doi:10.2147/OTT.S201025
109. Seachrist DD, Hannigan MM, Ingles NN, et al. The transcriptional repressor BCL11A promotes breast cancer metastasis. *J Biol Chem*. 2020;295:11707-11719. doi:10.1074/jbc.RA120.014018
110. Zhu Z, Zhang X, Guo H, Fu L, Pan G, Sun Y. CXCL13-CXCR5 axis promotes the growth and invasion of colon cancer cells via PI3K/AKT pathway. *Mol Cell Biochem*. 2015;400:287-295. doi:10.1007/s11010-014-2285-y
111. Wu B, Chen M, Gao M, et al. Down-regulation of lncTCF7 inhibits cell migration and invasion in colorectal cancer via inhibiting TCF7 expression. *Hum Cell*. 2019;32:31-40. doi:10.1007/s13577-018-0217-y
112. Wang SM, Tie J, Wang WL, et al. POU2F2-oriented network promotes human gastric cancer metastasis. *Gut*. 2016;65:1427-1438. doi:10.1136/gutjnl-2014-308932
113. Yi T, Zhou X, Sang K, Huang X, Zhou J, Ge L. Activation of lncRNA lncSLC4A1-1 induced by H3K27 acetylation promotes the development of breast cancer via activating CXCL8 and NF-kB pathway. *Artif Cells Nanomed Biotechnol*. 2019;47:3765-3773. doi:10.1080/21691401.2019.1664559
114. Lan Y, Han J, Wang Y, et al. STK17B promotes carcinogenesis and metastasis via AKT/GSK-3β/Snail signaling in hepatocellular carcinoma. *Cell Death Dis*. 2018;9:236. doi:10.1038/s41419-018-0262-1
115. Appert-Collin A, Bennasroune A, Jeannesson P, et al. Role of LRP-1 in cancer cell migration in 3-dimensional collagen matrix. *Cell Adh Migr*. 2017;11:316-326. doi:10.1080/19336918.2016.1215788
116. Kairouz R, Parmar J, Lyons RJ, Swarbrick A, Musgrove EA, Daly RJ. Hormonal regulation of the Grb14 signal modulator and its role in cell cycle progression of MCF-7 human breast cancer cells. *J Cell Physiol*. 2005;203:85-93. doi:10.1002/jcp.20199
117. Diez-Bello R, Jardin I, Lopez JJ, et al. (-)-Oleocanthal inhibits proliferation and migration by modulating Ca2+ entry through TRPC6 in breast cancer cells. *Biochim Biophys Acta Mol Cell Res*. 2019;1866:474-485. doi:10.1016/j.bbamcr.2018.10.010
118. Xue M, Tao W, Yu S, et al. lncRNA ZFPM2-AS1 promotes proliferation via miR-18b-5p/VMA21 axis in lung adenocarcinoma. *J Cell Biochem*. 2020;121:313-321. doi:10.1002/jcb.29176
119. Abo-Elfadl MT, Gamal-Eldeen AM, Ismail MF, Shahin NN. Silencing of the cytokine receptor TNFRSF13B: a new therapeutic target for triple-negative breast cancer. *Cytokine*. 2020;125:154790. doi:10.1016/j.cyto.2019.154790
120. Li J, Xu X, Wei C, Liu L, Wang T. Long noncoding RNA NORAD regulates lung cancer cell proliferation, apoptosis, migration, and invasion by the miR-30a-5p/ADAM19 axis. *Int J Clin Exp Pathol*. 2020;13:1-13.
121. Zhao J, Cheng L. Long non-coding RNA CCAT1/miR-148a axis promotes osteosarcoma proliferation and migration through regulating PIK3IP1. *Acta Biochim Biophys Sin (Shanghai)*. 2017;49:503-512. doi:10.1093/abbs/gmx041
122. Leite FA, Lira RC, Fedatto PF, et al. Low expression of HLA-DRA, HLA-DPA1, and HLA-DPB1 is associated with poor prognosis in pediatric adrenocortical tumors (ACT). *Pediatr Blood Cancer*. 2014;61:1940-1948. doi:10.1002/pbc.25118
123. Feng Y, Guo C, Wang H, et al. Fibrinogen-like protein 2 (FGL2) is a novel biomarker for clinical prediction of human breast cancer. *Med Sci Monit*. 2020;26:e923531. doi:10.12659/MSM.923531
124. Wang S, Xu L, Che X, et al. E3 ubiquitin ligases Cbl-b and c-Cbl downregulate PD-L1 in EGFR wild-type non-small cell lung cancer. *FEBS Lett*. 2018;592:621-630. doi:10.1002/1873-3468.12985
125. Zhong XP, Kan A, Ling YH, et al. NCKAP1 improves patient outcome and inhibits cell growth by enhancing Rb1/p53 activation in hepatocellular carcinoma. *Cell Death Dis*. 2019;10:369. doi:10.1038/s41419-019-1603-4
126. Yokoyama-Mashima S, Yogosawa S, Kanegae Y, et al. Forced expression of DYRK2 exerts anti-tumor effects via apoptotic induction in liver cancer. *Cancer Lett*. 2019;451:100-109. doi:10.1016/j.canlet.2019.02.046
127. Guo H, Zhang B, Nairn AV, et al. O-Linked N-acetylglucosamine (O-GlcNAc) expression levels epigenetically regulate colon cancer tumorigenesis by affecting the cancer stem cell compartment via modulating expression of transcriptional factor MYBL1. *J Biol Chem*. 2017;292:4123-4137. doi:10.1074/jbc.M116.763201
128. Lawson J, Dickman C, MacLellan S, et al. Selective secretion of microRNAs from lung cancer cells via extracellular vesicles promotes CAMK1D-mediated tube formation in endothelial cells. *Oncotarget*. 2017;8:83913-83924. doi:10.18632/oncotarget.19996
129. Wang X, Ye M, Wu M, et al. RNF213 suppresses carcinogenesis in glioblastoma by affecting MAPK/JNK signaling pathway. *Clin Transl Oncol*. 2020;22:1506-1516. doi:10.1007/s12094-020-02286-x
130. Taheri M, Omrani MD, Noroozi R, Ghafouri-Fard S, Sayad A. Retinoic acid-related orphan receptor alpha (RORA) variants and risk of breast cancer. *Breast Dis*. 2017;37:21-25. doi:10.3233/BD-160248
131. Hoyo C, Murphy SK, Schildkraut JM, et al. IGF2R genetic variants, circulating IGF2 concentrations and colon cancer risk in African Americans and Whites. *Dis Markers*. 2012;32:133-141. doi:10.3233/DMA-2011-0865
132. Bai F, Xiao K. Prediction of gastric cancer risk: association between ZBTB20 genetic variance and gastric cancer risk in Chinese Han population. *Biosci Rep*. 2020;40:BSR20202102. doi:10.1042/BSR20202102
133. Hope C, Emmerich PB, Papadas A, et al. Versican-derived matrikines regulate Batf3-dendritic cell differentiation and promote T cell infiltration in colorectal cancer. *J Immunol*. 2017;199:1933-1941. doi:10.4049/jimmunol.1700529
134. Bai X, Wang W, Zhao P, et al. LncRNA CRNDE acts as an oncogene in cervical cancer through sponging miR-183 to regulate CCNB1 expression. *Carcinogenesis*. 2020;41:111-121. doi:10.1093/carcin/bgz166
135. Zienert E, Eke I, Aust D, Cordes N. LIM-only protein FHL2 critically determines survival and radioresistance of pancreatic cancer cells. *Cancer Lett*. 2015;364:17-24. doi:10.1016/j.canlet.2015.04.019
136. Yang J, Chen Z, Liu N, Chen Y. Ribosomal protein L10 in mitochondria serves as a regulator for ROS level in pancreatic cancer cells. *Redox Biol*. 2018;19:158-165. doi:10.1016/j.redox.2018.08.016
137. Xie F, Huang Q, Wang C, et al. Downregulation of long noncoding RNA SNHG14 suppresses cell proliferation and invasion by regulating EZH2 in pancreatic ductal adenocarcinoma (PDAC). *Cancer Biomark*. 2020;27:357-364. doi:10.3233/CBM-190908
138. Li SS, Jiang WL, Xiao WQ, et al. KMT2D deficiency enhances the anti-cancer activity of L48H37 in pancreatic ductal adenocarcinoma. *World J Gastrointest Oncol*. 2019;11:599-621. doi:10.4251/wjgo.v11.i8.599
139. Zhu G, Zhou L, Liu H, Shan Y, Zhang X. MicroRNA-224 promotes pancreatic cancer cell proliferation and migration by targeting the

TXNIP-mediated HIF1α pathway. *Cell Physiol Biochem*. 2018;48:1735-1746. doi:10.1159/000492309

140. Zhang KD, Hu B, Cen G, et al. MiR-301a transcriptionally activated by HIF-2α promotes hypoxia-induced epithelial-mesenchymal transition by targeting TP63 in pancreatic cancer. *World J Gastroenterol*. 2020;26:2349-2373. doi:10.3748/wjg.v26.i19.2349
141. Wuebben EL, Wilder PJ, Cox JL, et al. SOX2 functions as a molecular rheostat to control the growth, tumorigenicity and drug responses of pancreatic ductal adenocarcinoma cells. *Oncotarget*. 2016;7:34890-34906. doi:10.18632/oncotarget.8994
142. Muthalagu N, Monteverde T, Raffo-Iraolagoitia X, et al. Repression of the type I interferon pathway underlies MYC- and KRAS-dependent evasion of NK and B cells in pancreatic ductal adenocarcinoma. *Cancer Discov*. 2020;10:872-887. doi:10.1158/2159-8290.CD-19-0620
143. Wang Z, Chen Y, Lin Y, et al. Novel crosstalk between KLF4 and ZEB1 regulates gemcitabine resistance in pancreatic ductal adenocarcinoma. *Int J Oncol*. 2017;51:1239-1248. doi:10.3892/ijo.2017.4099
144. Hu L, Fang L, Zhang ZP, Yan ZL. TPM1 is a novel predictive biomarker for gastric cancer diagnosis and prognosis. *Clin Lab*. 2020;66. doi:10.7754/Clin.Lab.2019.190235
145. Chen H, Fan Y, Xu W, et al. Exploration of miR-1202 and miR-196a in human endometrial cancer based on high throughout gene screening analysis. *Oncol Rep*. 2017;37:3493-3501. doi:10.3892/or.2017.5596